Space Charge Induced Beam Emittance Growth and Halo Formation

Space charge effect resulted in beam emittance growth are typically can be divided by two classes:

(i) single particle dynamics in collective space charge field of “pseudo” multipoles (incoherent space charge effects):

- Space charge aberrations
- “Free Energy” effect
- Excitation of nonlinear resonances
- Particle-core interaction

(ii) instabilities and resonances of beam distribution (coherent space charge effects).

Effect of Space Charge Aberration on Beam Emittance

Space charge density and space charge field of the beam with Gaussian distribution are given by

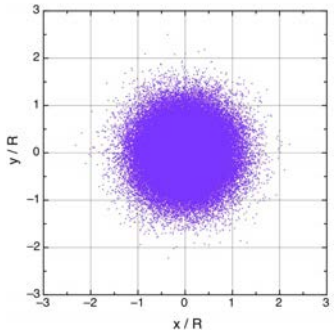

$$\rho(r_o) = \frac{2I}{\pi R_o^2 \beta c} \; exp(-2\frac{r_o^2}{R_o^2})$$

$$E_b = \frac{I}{2\pi \varepsilon_o \beta c}\frac{1}{r_o}[\,1 - exp(-2\frac{r_o^2}{R_o^2})]$$

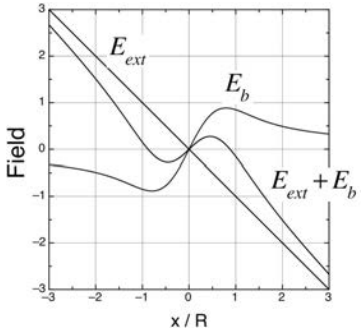

Nonlinear function in space charge field is expanded as

$$f(r_o) = 1 - exp(-2\frac{r_o^2}{R_o^2}) \approx 2\frac{r_o^2}{R_o^2} - 2\frac{r_o^4}{R_o^4} + \ldots$$

At the initial stage of beam emittance growth we can assume, that particle radius is unchanged, while the slope of the trajectory is changed. It gives us the nonlinear transformation:

$$r = r_o$$

$$r' = r_o' + \frac{2zP^2}{R_o^2} r_o - \frac{2zP^2}{R_o^4} r_o^3$$

where $P^2 = \frac{2I}{I_c \beta^3 \gamma^3}$ is the generalized perveance, $I_c = 4\pi\varepsilon_o mc^3/q$ is the characteristic beam current.

Effect of Space Charge Aberration on Beam Emittance

Parameter υ, which determines effect of spherical abberation on beam emittance is

$$\frac{C_\alpha R_o^4}{f\text{э}} = \frac{4}{\beta^3\gamma^3}\frac{I}{I_c}\frac{z}{\text{э}}$$

Therefore, space charge induced beam emittance growth in free space is:

$$\frac{\text{э}_{eff}}{\text{э}} = \sqrt{1+\bar{K}\left(\frac{I}{I_c\beta^3\gamma^3}\frac{z}{\text{э}}\right)^2}$$

Parameter $\bar{K}$ was determined numerically for different distributins. Results are summarized in Table. As follows from above equation, initial emittance growth does not depend on initial beam radius.

Distribution	Coeff. $\bar{K}$
KV	0
Water Bag	0.094
Parabolic	0.187
Gaussian	0.55

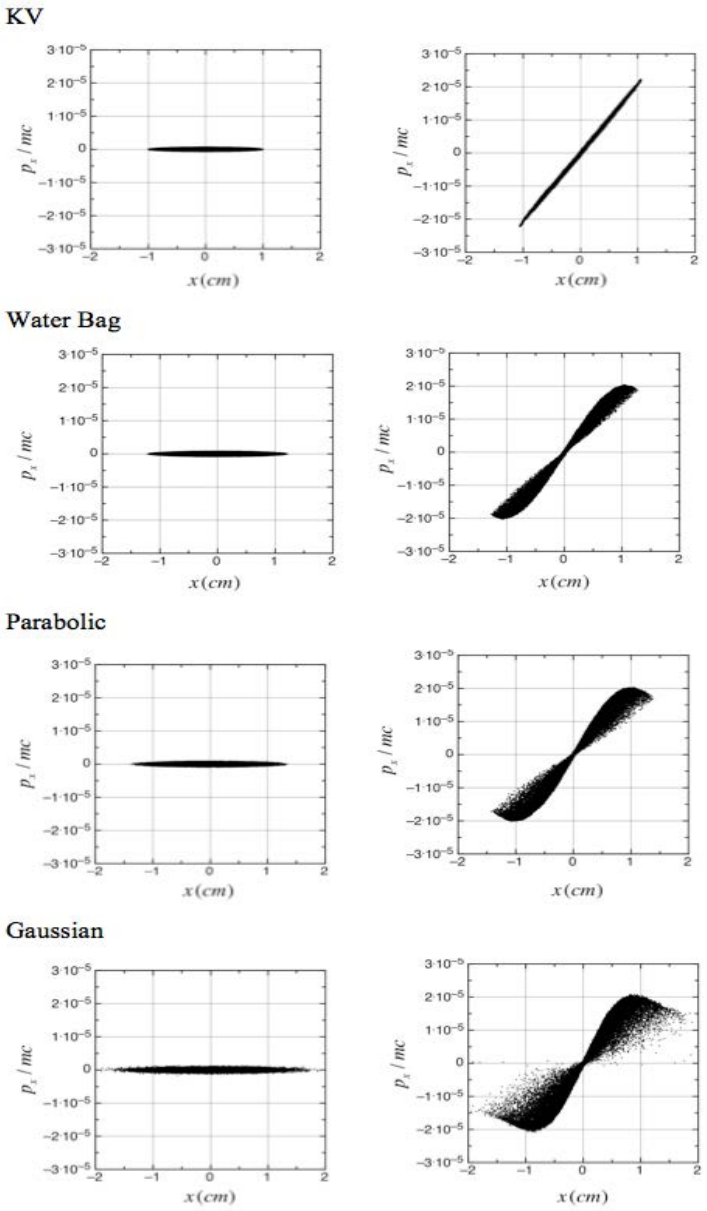

Experimental Observation of Effect of Nonlinear Space Charge Forces on Beam Emittance

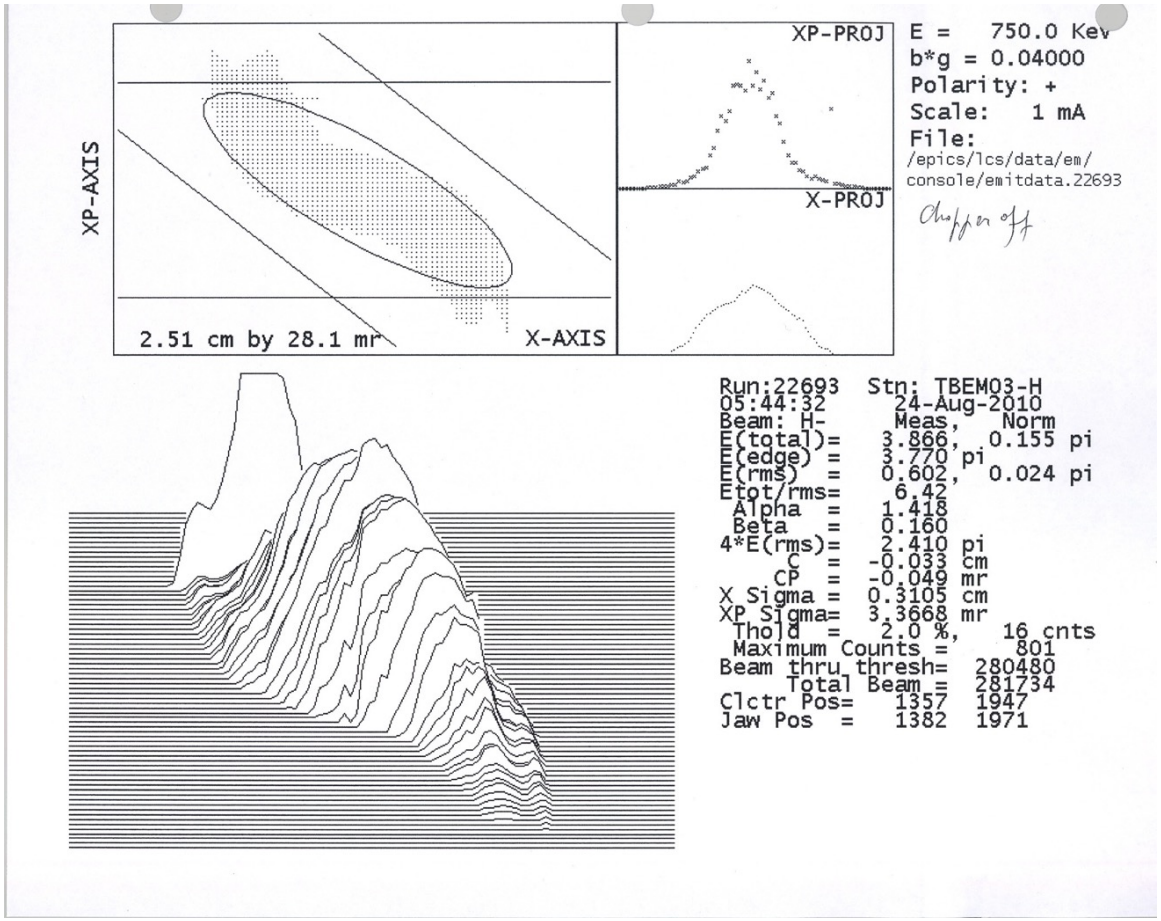

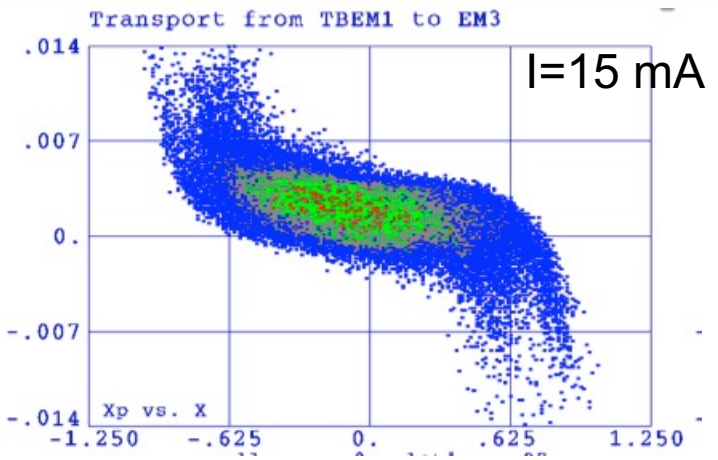

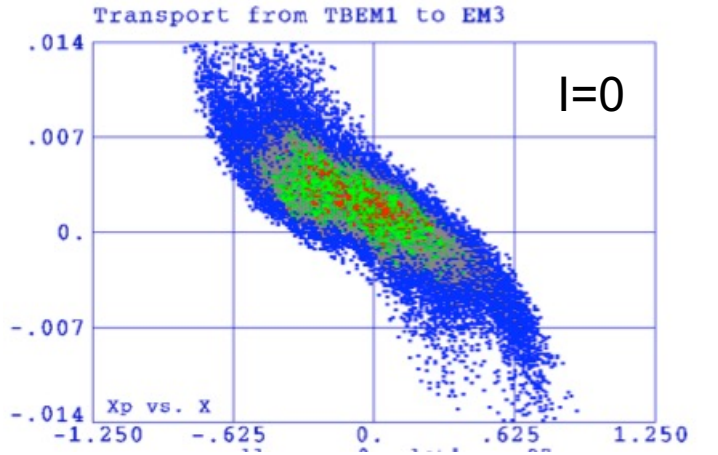

(Y.B. et al, Proc. of PAC2011, p. 64)

Effect of Elliptical Cross Section on Beam Emittance Growth

Suppose that the density is parabolic, given by

$$n(x,y) = \frac{2N_1}{\pi ab}\left[1 - \frac{x^2}{a^2} - \frac{y^2}{b^2}\right],$$

within the boundary of the ellipse defined by

$$\frac{x^2}{a^2} + \frac{y^2}{b^2} = 1 .$$

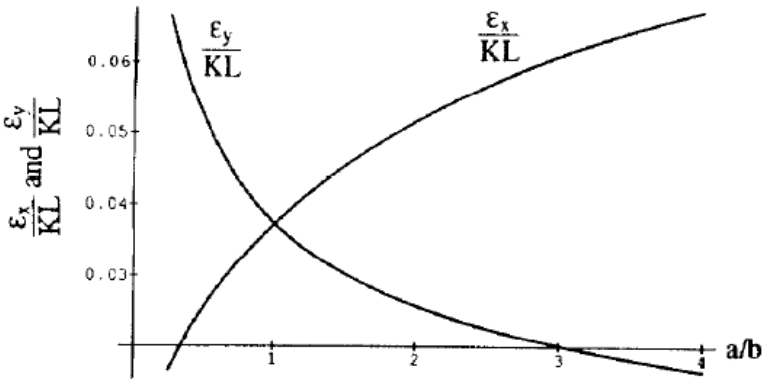

Figure 4. Final rms emittance values versus ellipse-aspect ratio a/b for a beam with parabolic density.

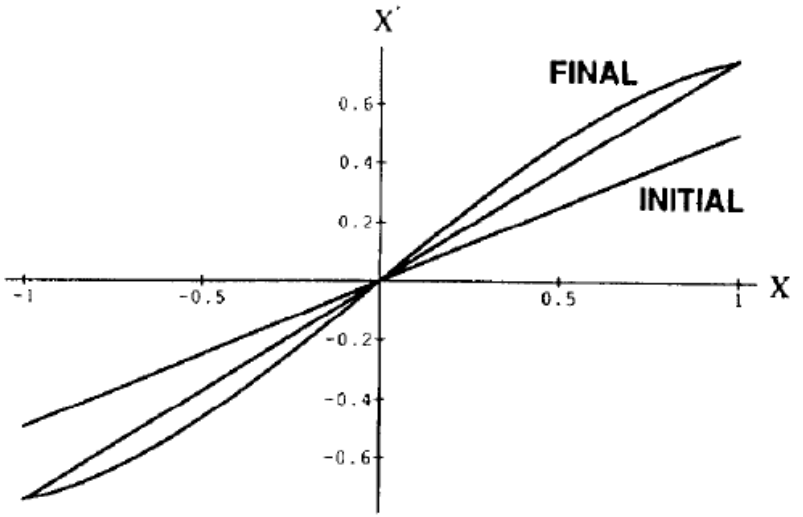

Figure 3. Effect of space charge from a parabolic density on an initial zero-emittance beam. The initial and final phase-space distributions are shown.

$$\varepsilon_x = KL\frac{a}{b}\sqrt{\frac{1}{432}\frac{\left(\frac{2a}{b}+1\right)^2}{\left\{1+\frac{a}{b}\right\}^4} + \frac{7}{720}\frac{1}{\left\{1+\frac{a}{b}\right\}^4} - \frac{1}{360}\frac{\left(\frac{2a}{b}+1\right)}{\left\{1+\frac{a}{b}\right\}^4}} .$$

(T.Wangler, P.Lapostolle, A.Lombardi, PAC 1993, p.3606)

Space Charge Induced Beam Emittance Growth

Drift

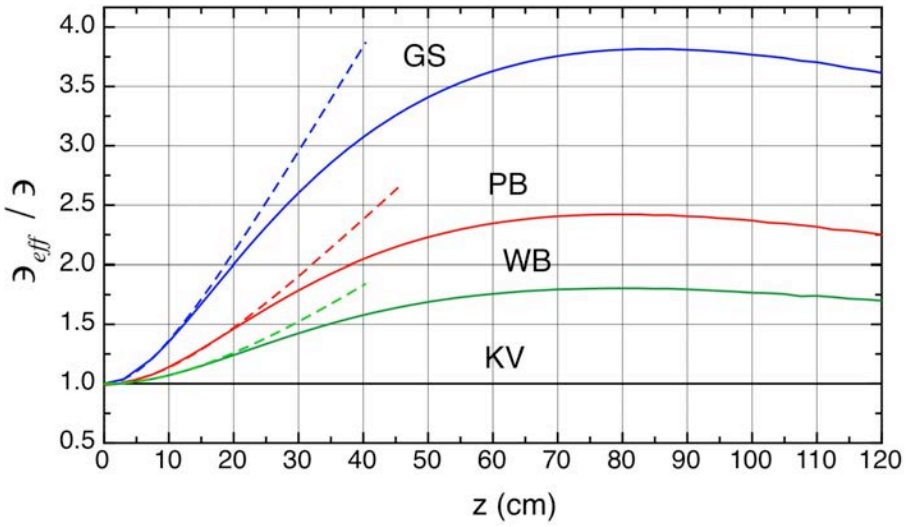

FODO Channel

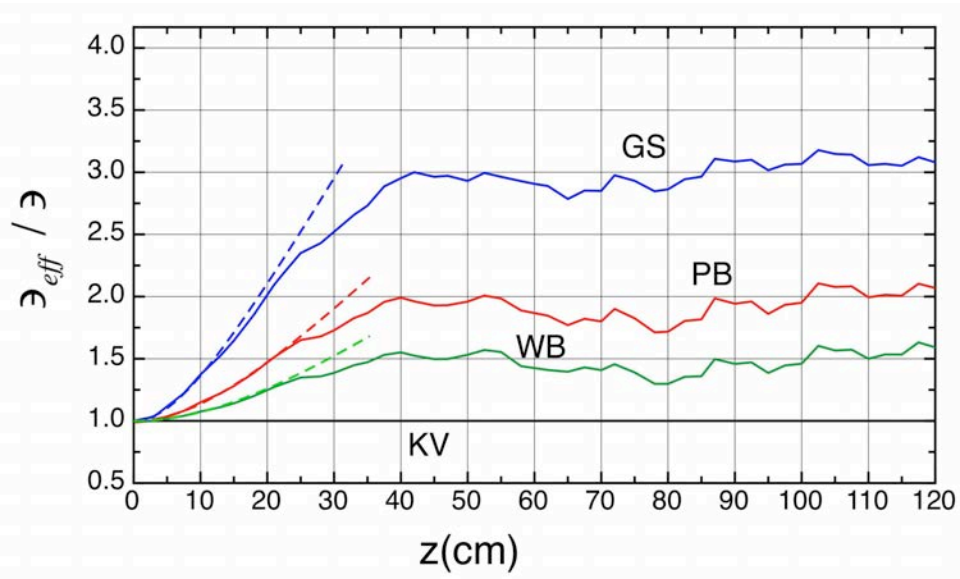

Emittance growth of a 50 keV proton beam with current I = 20 mA and unnormalized emittance 4.64 π cm mrad in drift space and in FODO focusing channel for different beam distributions: (solid) simulations, (dotted) aberration approximation.

Space Charge Induced Beam Emittance Growth in a Focusing Channel ("Free Energy" Effect)

z = 0

z = 30 cm

z = 104 cm

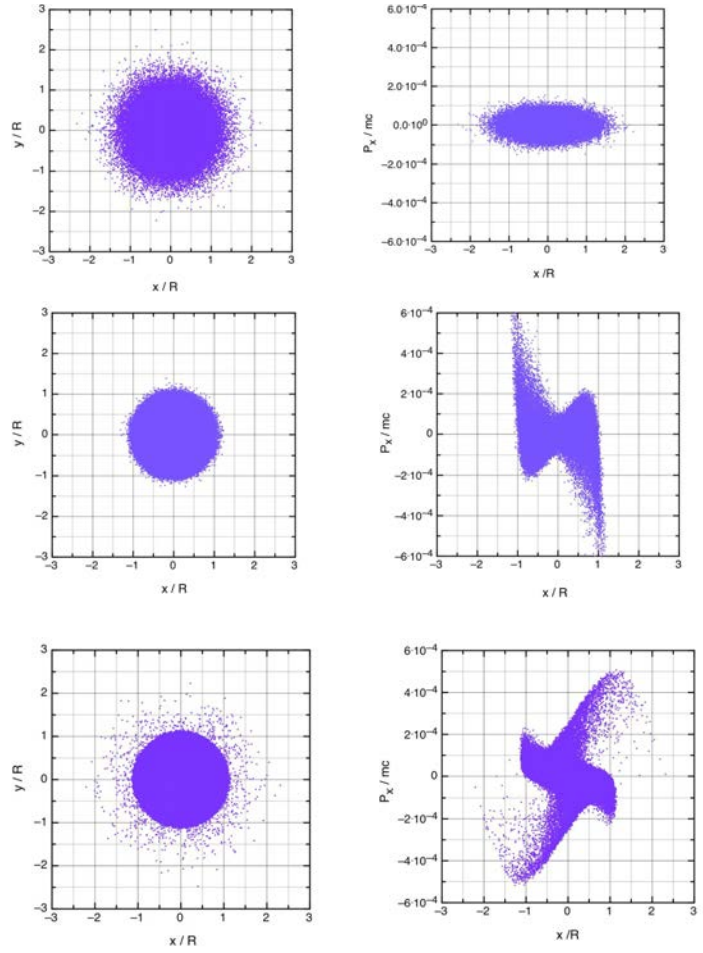

Fig. 3.7. Injection of 135 keV, 100 mA, 0.07 π cm mr ad proton beam with Gaussian distribution in a focusing channel with linear field. It results in (a) beam uniforming
(b) beam emittance growth
(c) halo formation.

Application of Poynting's Theorem

Conservation of energy for electromagnetic field (Umov-Poynting's theorem)

$$\oint_S [\vec{E},\vec{H}]\,d\vec{S} = -\frac{d}{dt}\int_V \left(\frac{\mu_o H^2}{2} + \frac{\varepsilon_o E^2}{2}\right) dV - \int_V \vec{j}\vec{E}\,dV$$

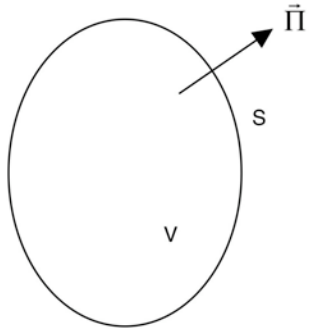

Expression on the left side is an integral of Poynting's vector $\vec{\Pi} = [\vec{E},\vec{H}]$ over surface *S* surrounding volume *V* and is equal to the power of electromagnetic irradiation, or energy of electromagnetic field coming through the surface *S* per second. Because beam in propagating in conducting tube, no energy is transferred through it. The first integral in right side of Poynting theorem is a change of energy of electromagnetic field per second:

$$\frac{d}{dt}\int_V \left(\frac{\mu_o H^2}{2} + \frac{\varepsilon_o E^2}{2}\right) dV = \frac{dW}{dt}$$

Second term in right side of Poynting theorem is a change of kinetic energy of the beam per second:

$$\int_V \vec{j}\vec{E}\,dV = \frac{d}{dt}\sum_{i=1}^{N} W_{kin}$$

For non-relativistic case (no magnetic field):

$$\frac{d}{dt}\left(\frac{\varepsilon_o}{2}\int E^2\,dV + \sum_{i=1}^{N} W_{kin}\right) = 0$$

Emittance Growth due to Charge Redistribution

where E is the total electrostatic field in the structure, and W_{kin} is the kinetic energy of particle:

$$W_{kin} = mc^2\sqrt{1+\frac{p_x^2+p_y^2+p_z^2}{(mc)^2}} \approx mc^2(\gamma-1)+\frac{p_x^2+p_y^2}{2m\gamma} \qquad (3.62)$$

and summation is performed over all particles of the beam. Below consider only transverse particle motion and kinetic energy, associated with this motion. According to definition of rms beam values, kinetic energy of particles is:

$$\sum_{i=1}^{N} W_{kin} = \frac{N}{2m\gamma}\left[\langle p_x^2\rangle + \langle p_y^2\rangle\right]. \qquad (3.63)$$

where rms value of transverse momentum is $$\langle p_x^2\rangle = \left(\frac{mc\varepsilon}{2R}\right)^2. \qquad (3.64)$$

In a round beam rms values in both transverse directions are the same, $\langle p_x^2\rangle = \langle p_y^2\rangle$, therefore

$$\sum_{i=1}^{N} W_{kin} = N\frac{mc^2}{\gamma}\left(\frac{\varepsilon}{2R}\right)^2. \qquad (3.65)$$

Emittance Growth due to Charge Redistribution (cont.)

Finally, equation for conservation of total energy can be can be rewritten for matched beam ($R_f \approx R_o$) as

$$\frac{\varepsilon_f}{\varepsilon_i} = \sqrt{1 + \left(\frac{\mu_o^2}{\mu^2} - 1\right)\left(\frac{W_i - W_f}{W_o}\right)}$$

where initial, W_i, and final, W_f, energy stored in electrostatic field are

$$W_i = \frac{\varepsilon_o}{2}\int_o^\infty E_i^2\, dS \qquad W_f = \frac{\varepsilon_o}{2}\int_o^\infty E_f^2\, dS,$$

and normalization constant is

$$W_o = 2\pi\varepsilon_o\left(\frac{I}{I_c}\,\frac{mc^2}{q\beta\gamma}\right)^2$$

Emittance Growth due to Charge Redistribution (cont.)

Consider beam with initial Gaussian distribution. Initial total field E_i is given by:

$$E_i = \frac{mc^2}{qR\gamma}\frac{2I}{\beta\gamma I_c}\{-\frac{r}{R}+\frac{R}{r}[\,1 - exp(-\frac{2r^2}{R^2})\}\,. \qquad (3.73)$$

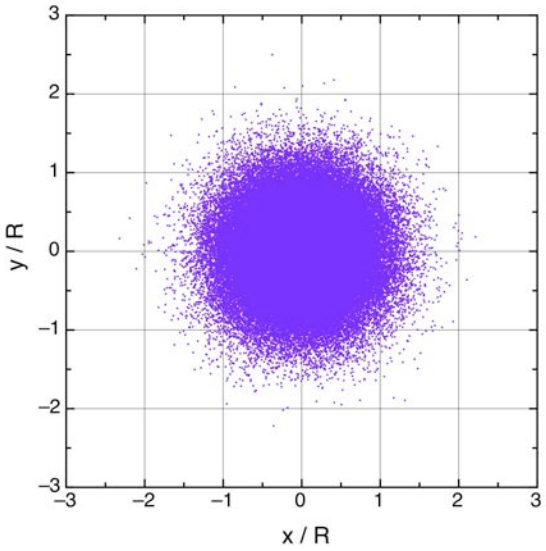

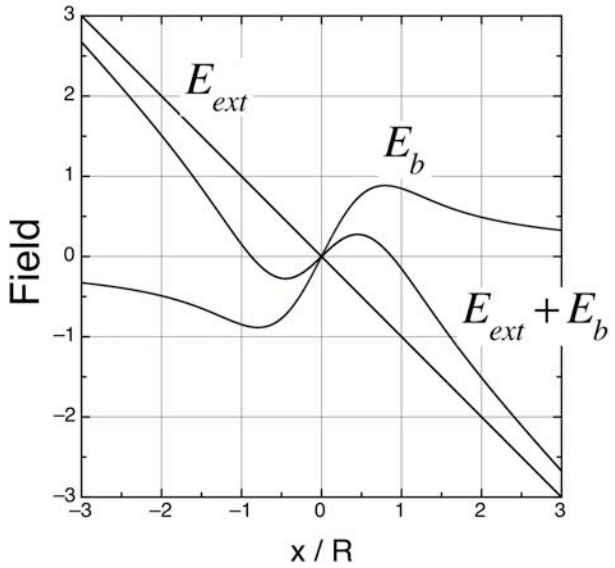

External focusing field E_{ext}, space charge field of Gaussian beam E_b, and total field E_{ext} + E_b at initial moment of time.

Emittance Growth due to Charge Redistribution (cont.)

Final beam distribution is close to uniform with the same value of beam radius R. It is a general property of space-charge dominated regime, that self-field of the beam almost compensates for external field within the beam. We can put $E_f \approx 0$ within the beam and $E_f = E_{ext} + E_b$ outside the beam

$$E_f = \begin{cases} 0, & r \le R \\ \dfrac{mc^2}{qR}\dfrac{2I}{\beta\gamma^2 I_c}\left(-\dfrac{r}{R}+\dfrac{R}{r}\right), & r > R \end{cases} . \qquad (3.74)$$

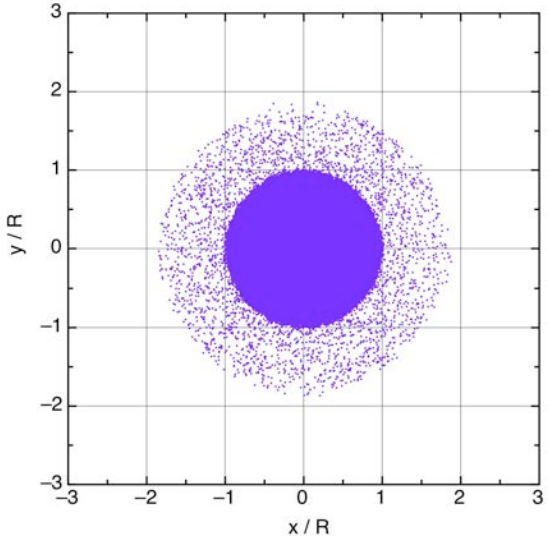

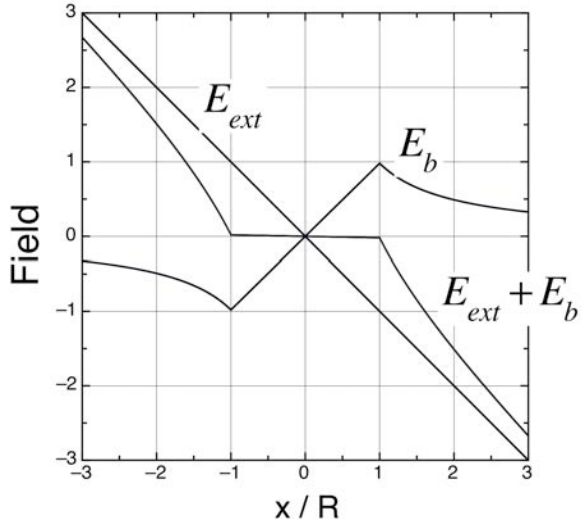

External focusing field E_{ext}, space charge field E_b, and total field $E_{ext} + E_b$ after beam uniforming.

Emittance Growth due to Charge Redistribution (cont.)

Calculation of "free energy" parameter for Gaussian beam gives:

$$\frac{W_f - W_i}{W_o} = \int_o^{\xi_{max}} [-\xi + \frac{1}{\xi}(1 - e^{-2\xi^2})]^2 \xi d\xi - \int_1^{\xi_{max}} (-\xi + \frac{1}{\xi})^2 \xi d\xi \approx 0.077$$

Free energy parameter for different beam distributions

4D Distribution	2D Projection	$\frac{W_i - W_f}{W_o}$
KV	ρ_o	0
Water Bag	$\rho_o(1-\frac{r^2}{R^2})$	0.01126
Parabolic	$\rho_o(1-\frac{r^2}{R^2})^2$	0.02366
Gaussian	$\rho_o \exp(-\frac{r^2}{R^2})$	0.077

Emittance Growth due to Charge Redistribution (cont.)

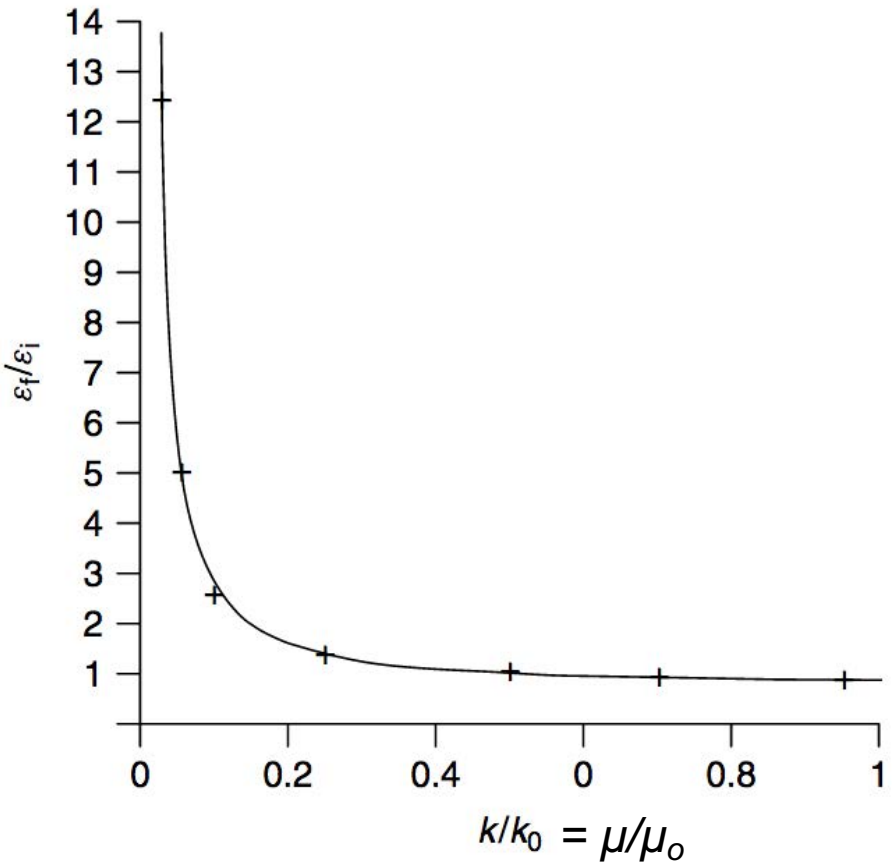

Final emittance growth ratio versus space charge tune depression for an initial Gaussian beam. Typical space charge tune depression in linacs $\mu / \mu_o > 0.4$.

Excitation of Single Particle Space-Charge Induced Nonlinear Resonances

Nonlinear components of oscillating space charge field can excite nonlinear resonances. Particle dynamics in focusing channel in presence of oscillation nonlinear field is determined by equation

$$\frac{d^2x}{d\tau^2} + \mu^2 x + \alpha_n(\tau)x^{n-1} = 0$$

Resonance is excited when particle trajectory is perturbed integer number of times *n* per one complete oscillation by a nonlinear field component of the order *n* . The lowest-order resonance is the parametric resonance of a linear oscillator (*n* = 2) described by Mathie equation.

Beam space charge field contains components of the order *n* = 2, 4, 6,.. Beam envelope oscillates with the period of focusing structure and constitute periodic perturbation of single-particle trajectory. Resonance condition for excitation of single particle nonlinear resonances:

$$\mu = \frac{360^o}{n}, \qquad n = 2, 3, 4,..$$

Single Particle Nonlinear Resonance of the 4th Order (n = 4)

Space-charge induces single-particle resonance of the 4th order in channels with $\mu = 360^o /4$. Because phase advance in presence of space charge forces is $\mu = \mu_s - \Delta\mu$, this resonance of the 4th order can be excited only in channels with $\mu_s > 90^o$ and $\mu_t < 90^o$. Accelerators are typically designed with $\mu_s < 90^o$ to avoid envelope resonances, and this 4th order resonance is not excited when $\mu_s < 90^o$.

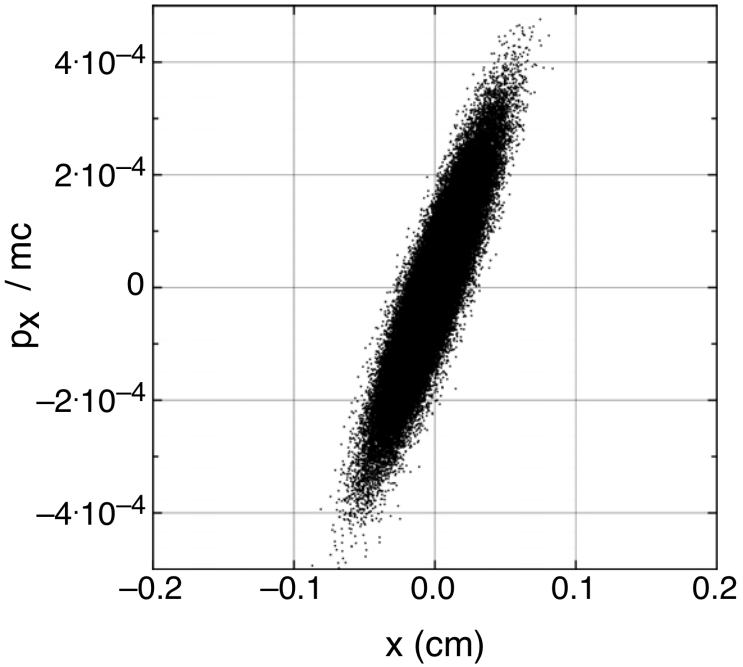

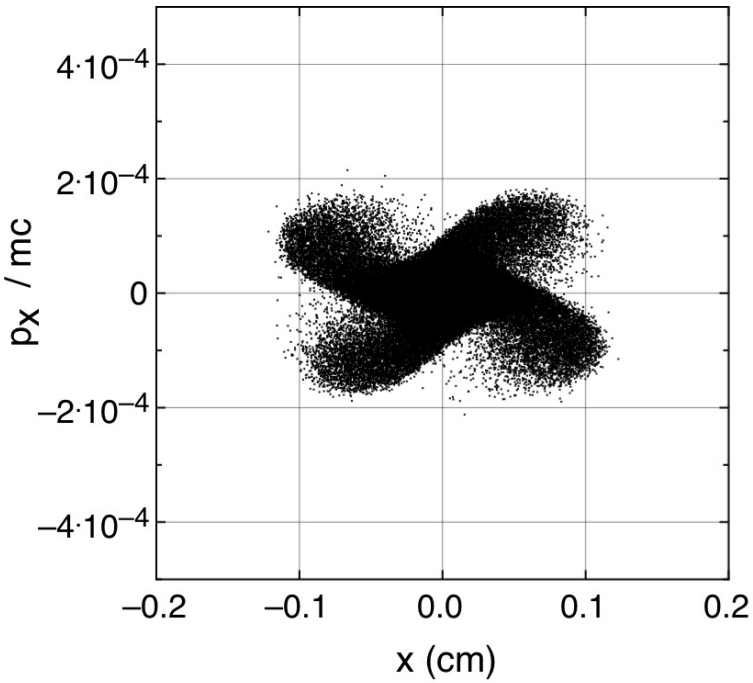

Excitation of nonlinear resonance of the 4th order in accelerator channel with $\mu_s = 93^o$, $\mu_t = 63^o$.

Experimental Observation of Space-Charge Driven Resonance of 4th Order in Linac (L. Groening et al, LINAC2010)

Matched beam envelope

$$R(s, \sigma_{env}) = R_o(\sigma_{env}) + \Delta R(\sigma_{env}) \cdot cos(\sigma_{env} s)$$

Radial electric field

$$E_r = \frac{18 \cdot I}{\pi \epsilon_o \cdot R(s)^2 \beta c} \left[r - \frac{r^3}{2R(s)^2} + O(r) \right]$$

Single-particle trajectory

or

$$r'' = -\sigma_{\perp,o}^2 r + \frac{e \cdot q}{A \cdot m_u} \cdot E_r$$

Disturbed oscillator with $\sigma_\perp$ *as* depressed phase advance

$$r'' + \sigma_\perp^2 r \sim r^3 \cdot e^{i\sigma_{env} s}$$

Resonance condition:

$$\sigma_{env} = 4\sigma_\perp.$$

Phase advance of the matched envelope is 360°, the resonance occurs at $\sigma_\perp$ = 90°

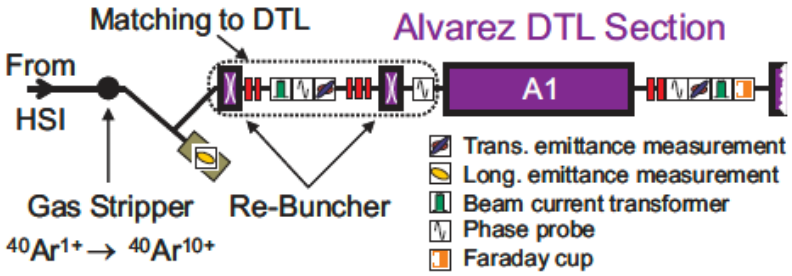

Figure 3: Schematic set-up of the experiments (not to scale).

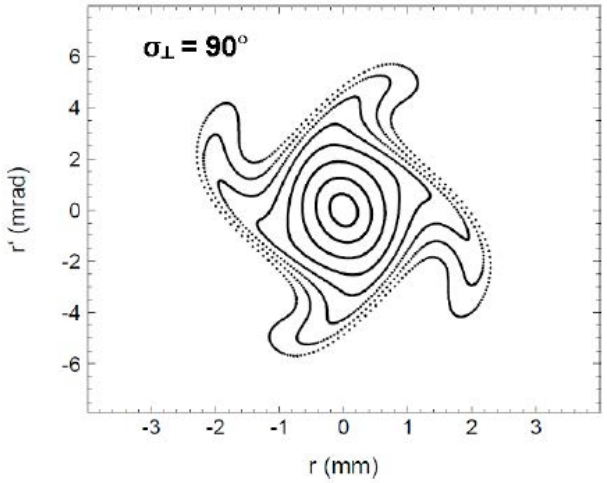

Figure 1: Distribution of particles at the exit of the periodic channel according to the radial particle-core model of the space charge driven transverse 4th-order resonance.

Experimental Observation of Space-Charge Driven Resonances (cont.)

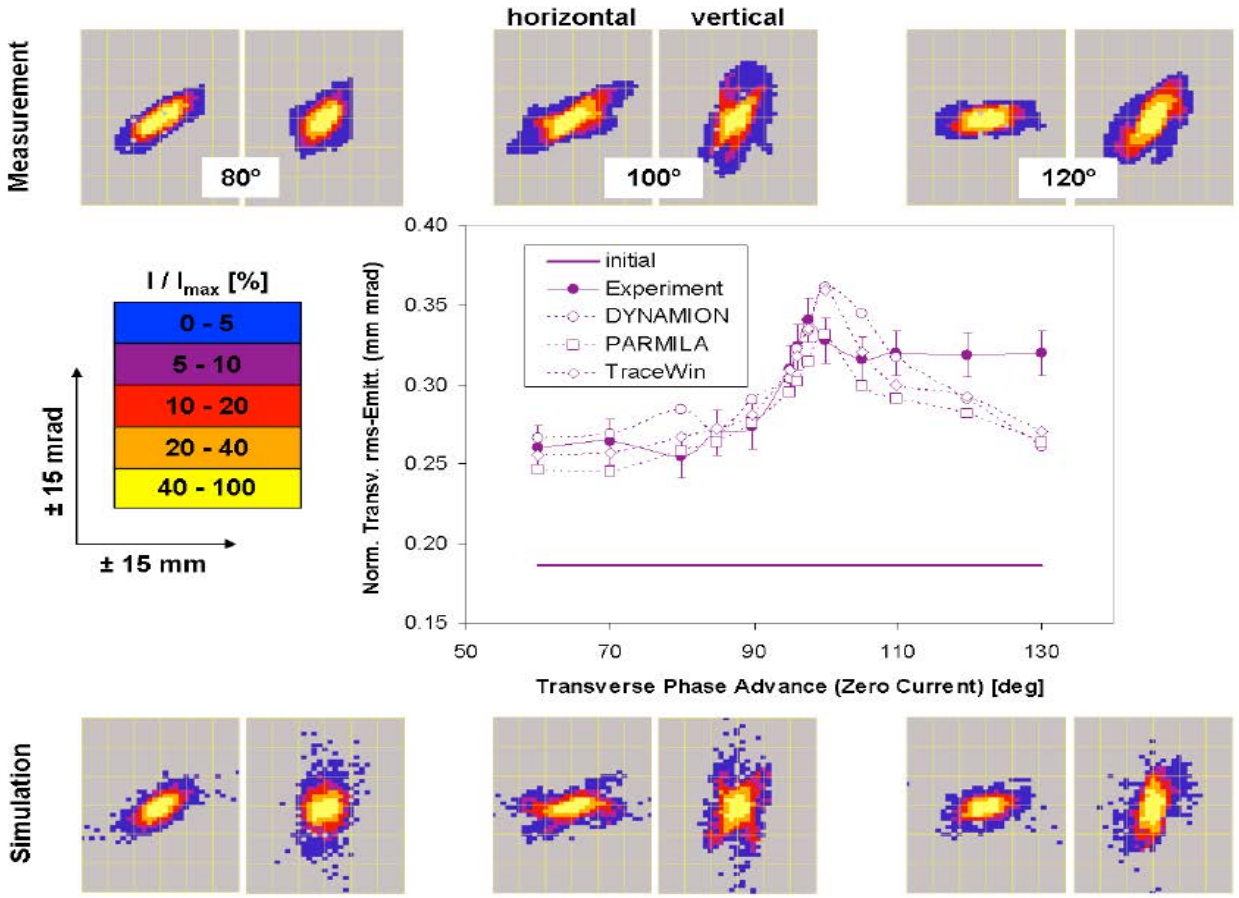

Figure 7: Upper and lower: phase space distributions at the exit of the first DTL tank as obtained from measurements and from the DYNAMION code for phase advances $\sigma_{\perp,o}$ of 80°, 100°, and 120°. Left (right) side distributions refer the horizontal (vertical) plane. The scale is ±15 mm and ±15 mrad. Fractional intensities refer to the phase space element including the highest intensity. Center: Mean of horizontal and vertical normalized rms emittance behind the first DTL tank as a function of the transverse zero current phase advance.

Halo Development in Particle-Core Interaction

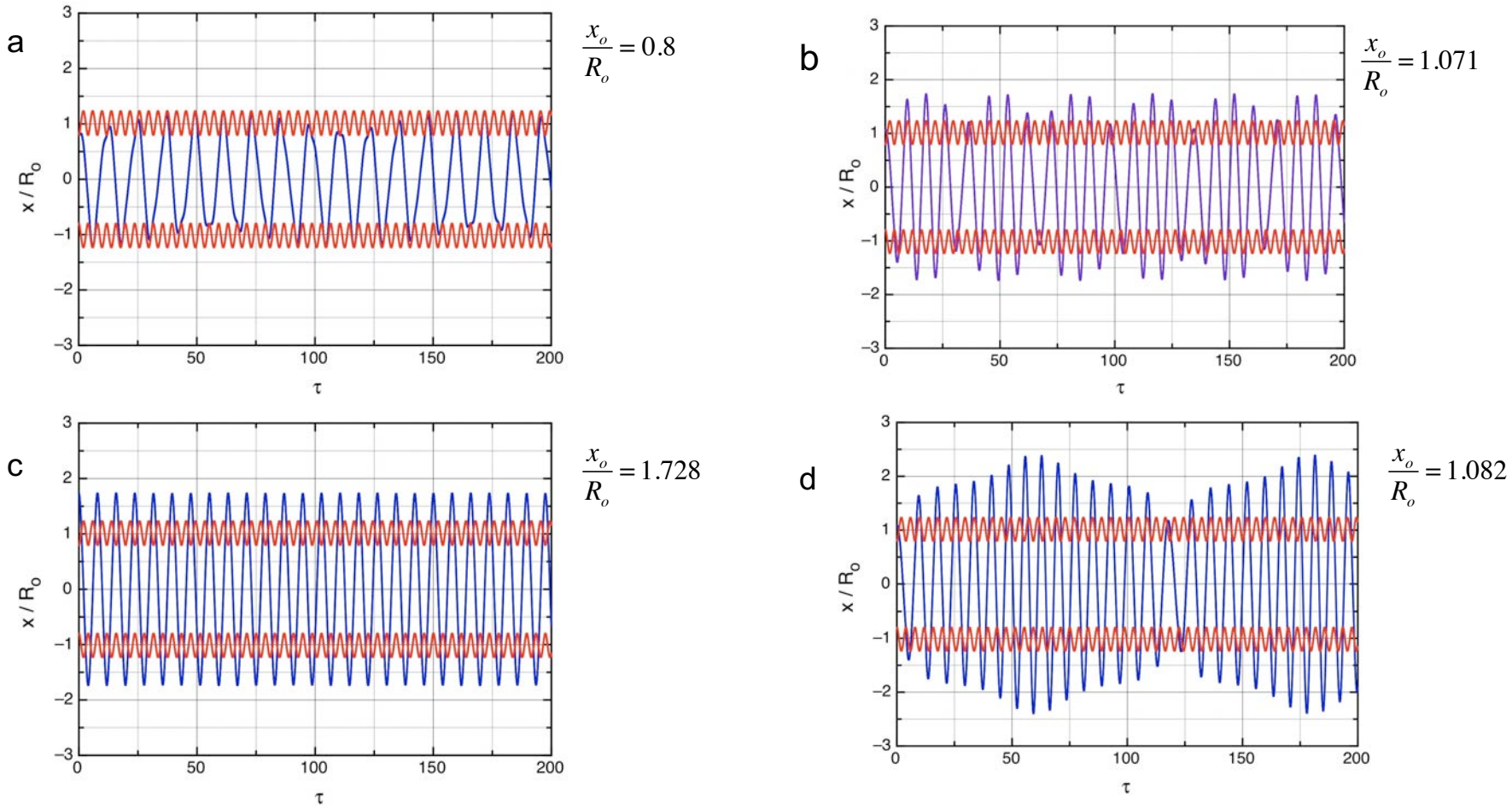

Envelope oscillations of the beam with space charge parameter b=3, amplitude Δ= 0.2 and single particle trajectories with initial conditions (a) x_o/R_o=0.8, (b) x_o/R_o =1.071, (c) x_o/R_o =1.728, (d) x_o/R_o =1.082.

Stroboscopic Particle Motion

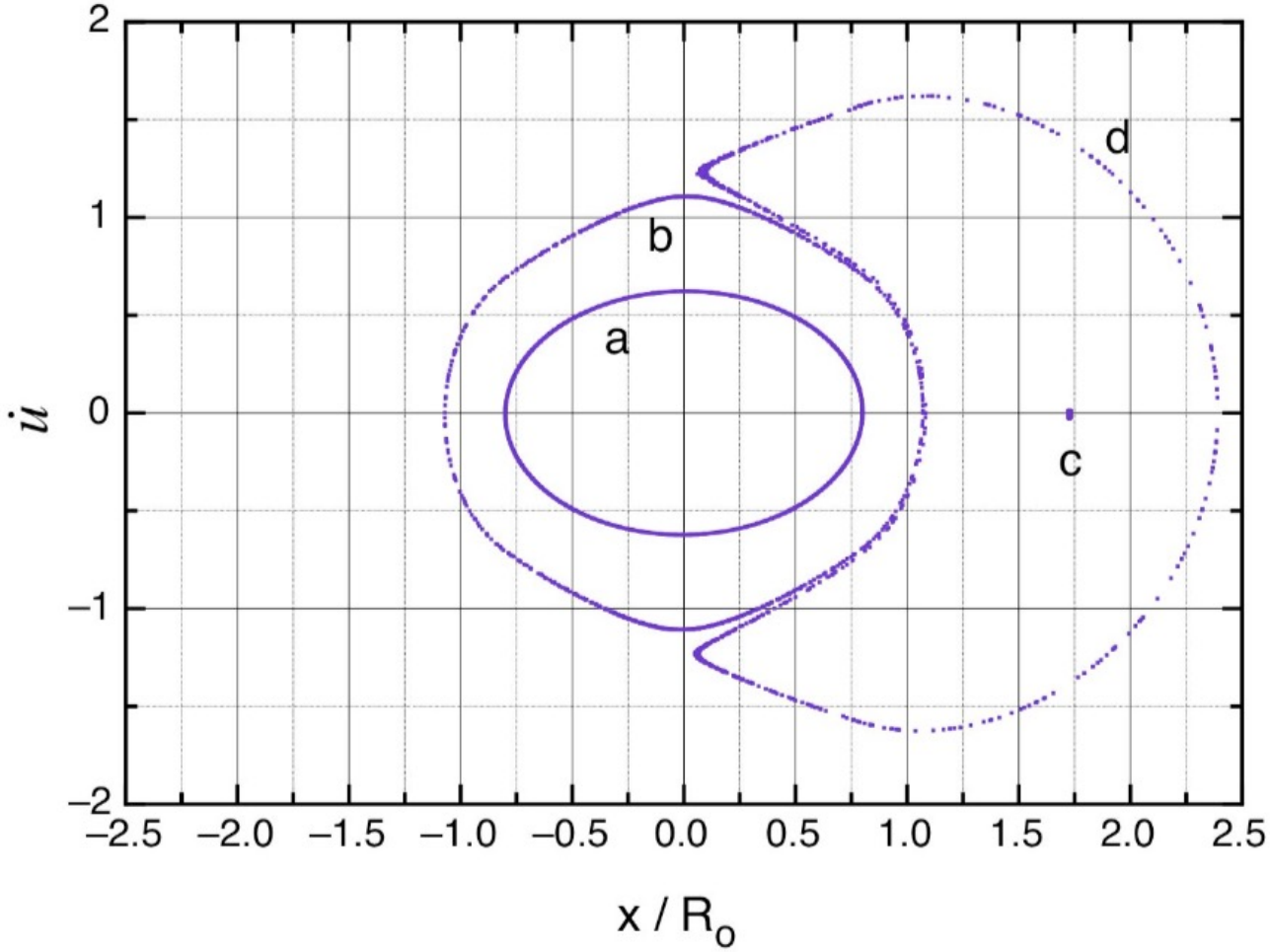

Stroboscopic particle trajectories at phase plane $(u, du/d\tau)$ taken after each two envelope oscillation periods: (a) x_o/R_o=0.8, (b) x_o/R_o =1.071, (c) x_o/R_o=1.728, (d) x_o/R_o =1.082.

Particle – Core Model

Dimensionless $r = \frac{R}{R_e}$ beam envelope (core) equation: $\frac{d^2 r}{d\tau^2} + r - \frac{1}{(1+b)r^3} - \frac{b}{(1+b)r} = 0$

Single particle equation of motion $u = \frac{x}{R_e}$

$$\frac{d^2 u}{d\tau^2} + u = \begin{cases} \frac{b}{(1+b)} \frac{u}{r^2}, & |u| \le r \\ \frac{b}{(1+b)u}, & |u| > r \end{cases}$$

Space charge parameter

$$\boxed{b = \frac{2}{\beta\gamma} \frac{I}{I_c} \frac{R_e^2}{\varepsilon^2}}$$

I beam current

$I_c = 4\pi\varepsilon_o mc^3 / q$ characteristic beam current

ε normalized beam emittance

β particles velocity,

γ particle energy

R_e radius of the equilibrium envelope

Small intensity beam $b \approx 0$

High intensity beam b >> 1

Approximation of Space Charge Field

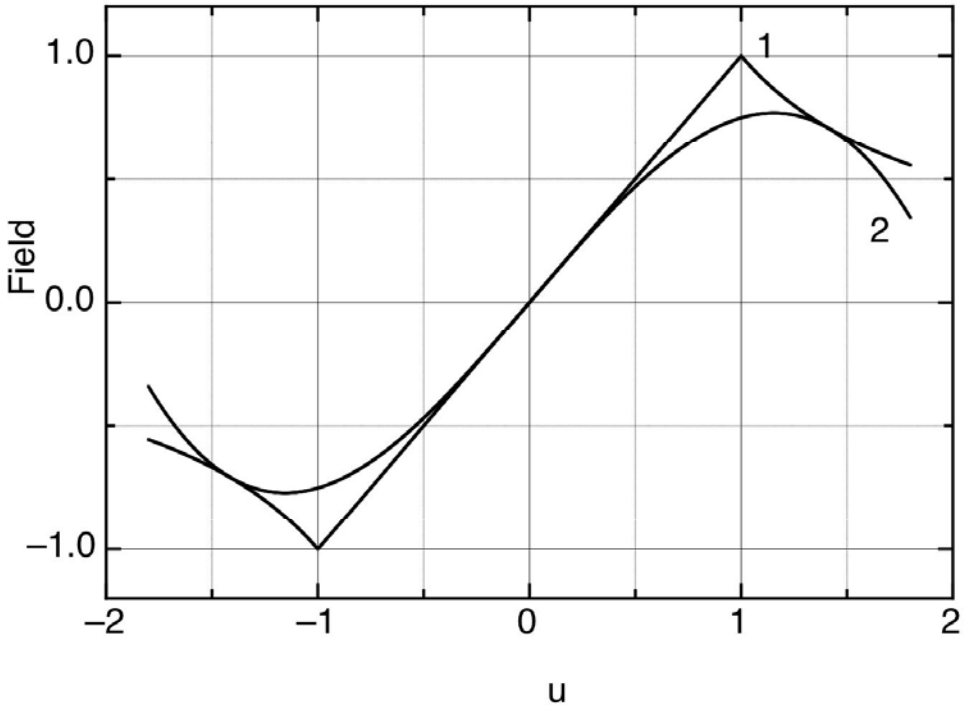

(1) Field of uniformly charged beam

$$F = \frac{b}{(1+b)}\begin{cases} \dfrac{u}{r^2}, & |u| \le r \\ \dfrac{1}{u}, & |u| > r \end{cases}$$

(2) Field approximation:

$$F = \frac{b}{(1+b)}\left(-\frac{u}{r^2} + \frac{u^3}{4}\right)$$

Mismatched Envelope Oscillation

Envelope equation $$\frac{d^2 r}{d\tau^2} + r - \frac{1}{(1+b)r^3} - \frac{b}{(1+b)r} = 0$$

Expansions $r = 1 + \vartheta$ $\quad \frac{1}{r} \approx 1 - \vartheta$ $\quad \frac{1}{r^3} \approx 1 - 3\vartheta$ $\quad \frac{d^2\vartheta}{d\tau^2} + 2\left(\frac{2+b}{1+b}\right)\vartheta = 0$

Equation for small deviation from equilibrium

$$r = 1 + \Delta\cos(2\Omega\tau)$$

Envelope oscillation frequency

$$2\Omega = \sqrt{2\left(\frac{2+b}{1+b}\right)}$$

For small intensity beam $b \approx 0$ $\quad r = 1 + \Delta\cos 2\tau$

For high intensity beam b >>1 $\quad r = 1 + \Delta\cos\sqrt{2}\tau$

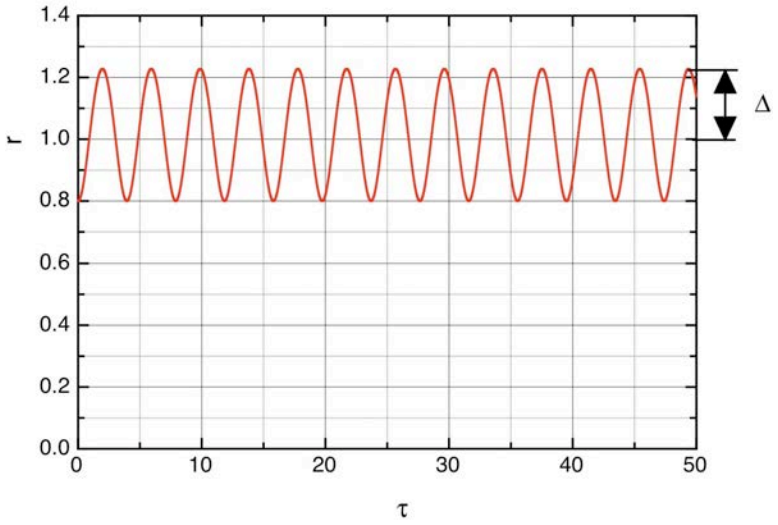

Harmonic Oscillator with Parametric Excitation for Single Particle Motion

With field approximation, equation of particle motion is

$$\frac{d^2u}{d\tau^2}+u-\left(\frac{b}{1+b}\right)\left[\frac{u}{(1+\Delta\cos 2\Omega\tau)^2}-\frac{u^3}{4}\right]=0$$

Using expansion

$$\frac{1}{(1+\Delta\cos 2\Omega\tau)^2}\approx 1-2\Delta\cos 2\Omega\tau$$

Equation of particle motion

$$\frac{d^2u}{d\tau^2}+u\left(\frac{1}{1+b}\right)(1+2b\Delta\cos 2\Omega\tau)+\left(\frac{b}{1+b}\right)\frac{u^3}{4}=0$$

Equation corresponds to Hamiltonian

$$\boxed{H=\frac{\dot{u}^2}{2}+\varpi^2\frac{u^2}{2}(1-h\cos 2\Omega\tau)+\alpha\frac{u^4}{4}}$$

with the following notations

$$\varpi^2=\frac{1}{1+b}\qquad h=-2b\Delta\qquad \alpha=\frac{b}{4\,(1+\,b)}$$

Canonical Transformation of Hamiltonian

Change the variables ($\dot{u}$, u) to new variables (Q, P) using a generating function

$$F_2(u,P,\tau) = \frac{uP}{\cos\Omega\tau} - \left(\frac{P^2}{2\varpi} + \varpi\frac{u^2}{2}\right) tg\Omega\tau$$

Relationships between variables are given by:

$$\begin{cases} Q = \dfrac{\partial F_2}{\partial P} = \dfrac{u}{\cos\,\Omega\,\tau} + \dfrac{P}{\varpi}\, tg\Omega\,\tau \\ \dot{u} = \dfrac{\partial F_2}{\partial u} = \dfrac{P}{\cos\,\Omega\,\tau} - \varpi\, u\, tg\Omega\,\tau \end{cases}$$

or

$$\begin{cases} u = Q\cos\Omega\,\tau + \dfrac{P}{\varpi}\sin\Omega\,\tau \\ \dot{u} = -\varpi\, Q\,\sin\Omega\,\tau + P\cos\,\Omega\,\tau \end{cases}$$

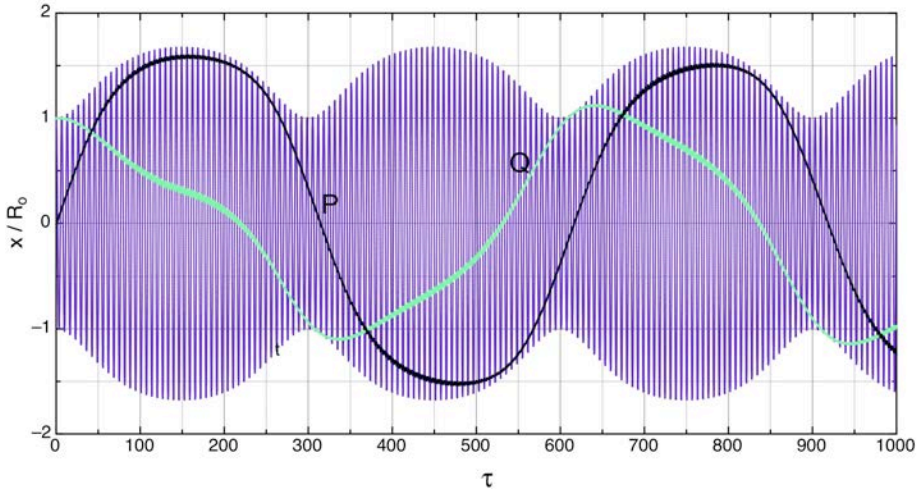

Averaged Hamiltonian

New Hamiltonian $$K = H + \frac{\partial F_2}{\partial \tau}$$

$$K = \frac{P^2}{2} + \varpi^2 \frac{Q^2}{2} - \frac{\varpi^2 h}{2}\left(Q\cos\Omega\tau + \frac{P}{\varpi}\sin\Omega\tau\right)^2 \cos 2\Omega\tau + \frac{\alpha}{4}\left(Q\cos\Omega\tau + \frac{P}{\varpi}\sin\Omega\tau\right)^4 - \frac{P^2\Omega}{2\varpi} - \frac{\Omega\varpi}{2}Q^2$$

After averaging all time-dependent terms over period of $2\pi/\Omega$

$$\bar{K} = \frac{\varpi^2\bar{Q}^2}{2}\left(1 - \frac{\Omega}{\varpi} - \frac{h}{4}\right) + \frac{\bar{P}^2}{2}\left(1 - \frac{\Omega}{\varpi} + \frac{h}{4}\right) + \frac{3}{32}\alpha\left(\bar{Q}^2 + \frac{\bar{P}^2}{\varpi^2}\right)^2$$

Second Canonical Transformation

Change variables $(\bar{Q},\bar{P})$ to action-angle variables $(J,\ \psi)$ using generating function

$$F_1(\bar{Q},\psi) = \frac{\varpi\ \bar{Q}^2}{2tg\psi}$$

Transformation is given by

$$\begin{cases} \bar{Q} = \sqrt{\dfrac{2J}{\varpi}}\sin\psi \\ \bar{P} = \sqrt{2J\varpi}\cos\psi \end{cases}$$

New Hamiltonian

$$\boxed{\bar{K} = \upsilon J + \kappa J^2 + 2\chi J\cos 2\psi}$$

with the following notations

$$\upsilon = \varpi - \Omega = \frac{\sqrt{2}-\sqrt{2+b}}{\sqrt{2(1+b)}} \qquad \kappa = \frac{3}{32}b \qquad \chi = -\frac{1}{4}\frac{b\Delta}{\sqrt{1+b}}$$

Nonlinear Parametric Resonance

Hamiltonian of averaged motion:

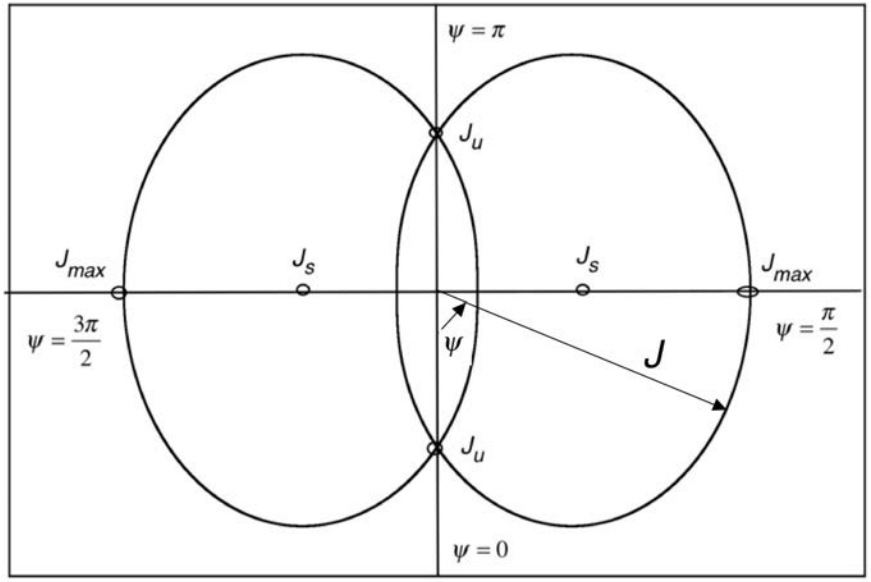

$$\bar{K} = \upsilon J + \kappa J^2 + 2\chi J \cos 2\psi$$

Maximum deviation of particle from the axis $\frac{x_{\max}}{R_e} = \sqrt{\frac{2J_{\max}}{\varpi}}$

$$J_{\max} = \frac{(-\upsilon + 2\chi) + \sqrt{8|\upsilon\chi|}}{2\kappa}$$

$$\frac{x_{\max}}{R_e} = \sqrt{\frac{32}{3}\frac{\sqrt{1+\frac{b}{2}} - 1 + \frac{b|\Delta|}{2} + \sqrt{2b|\Delta|(\sqrt{1+\frac{b}{2}} - 1)}}{b}}$$

Nonlinear Parametric Resonance

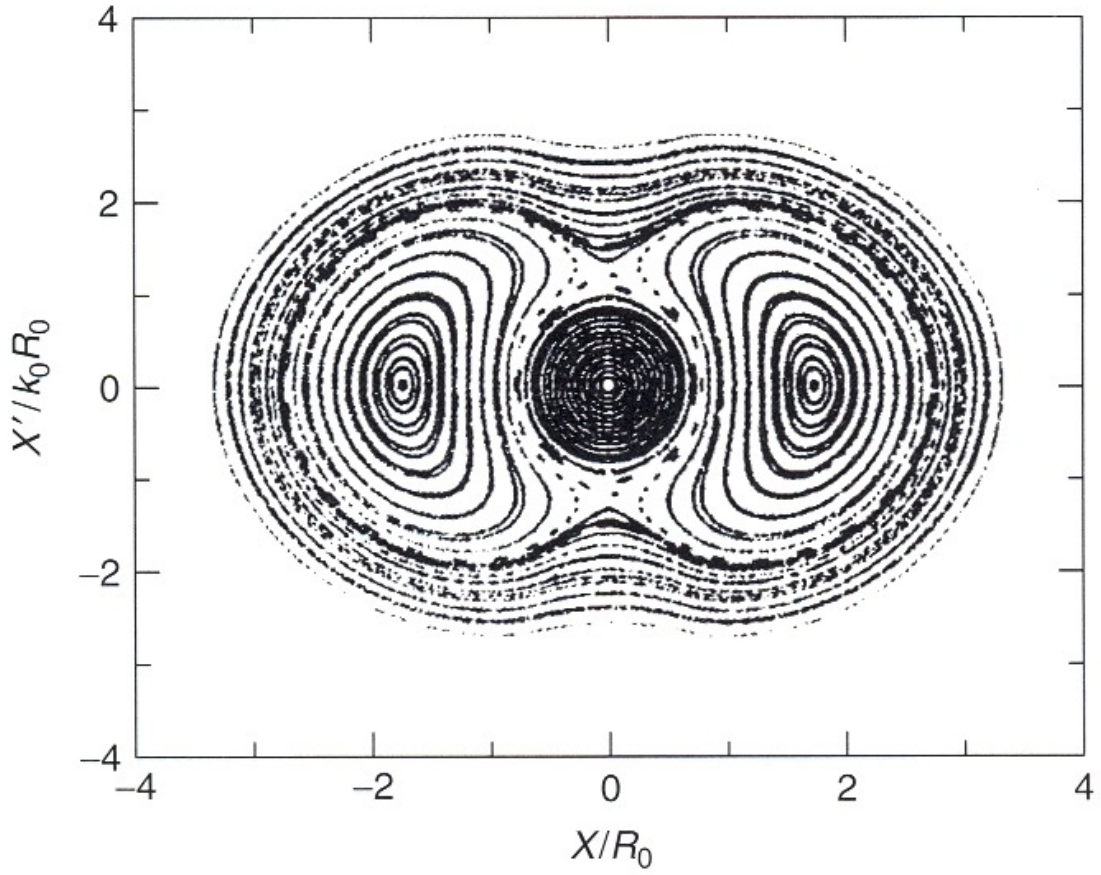

Figure 9.12 Stroboscopic plot obtained by taking snapshots of many independent particle trajectories, once per core-oscillation cycle at the phase of the core oscillation that gives the minimum core radius. Initial particle coordinates were defined on the x and x' axes.

Comparison of Analytical and Numerical Results

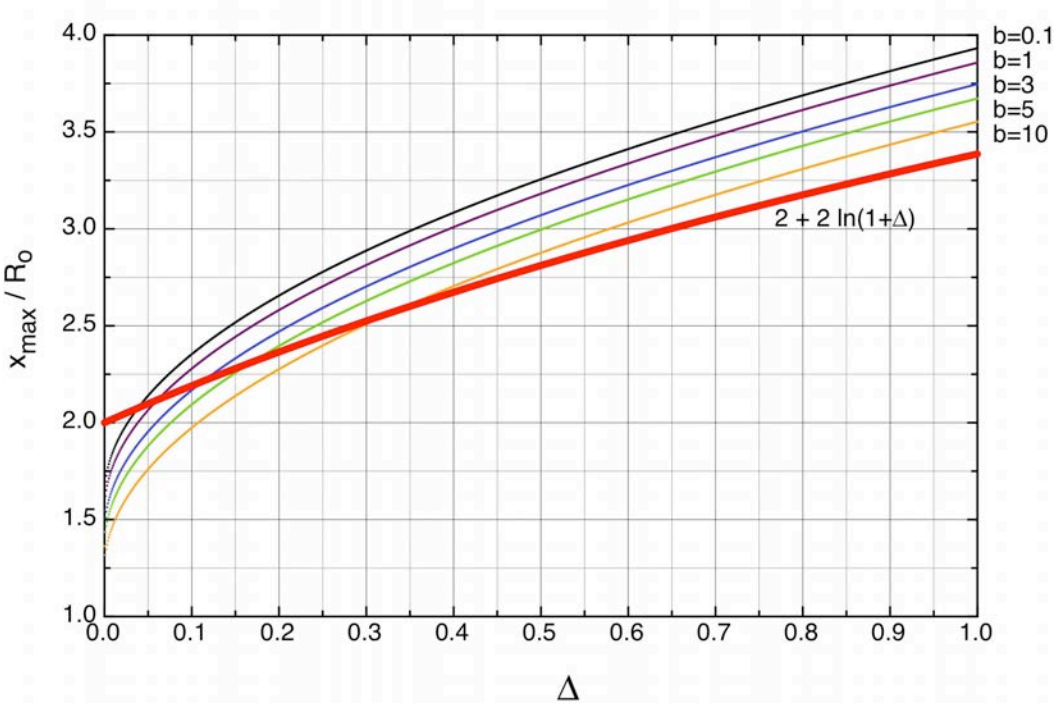

Maximum values of particle deviation from the axis as a function of amplitude of core oscillations (Y.B. NIM-A 618, 2010, p.37). (Red) model of Tom Wangler (*RF Linear Accelerators*, Wiley, 1998)

$$\frac{x_{\max}}{R_o/2} = A + B\ln(\mu)$$

where $A = B = 4$, $\mu = 1+\Delta$.

LANL Beam Halo Experiment (2002)

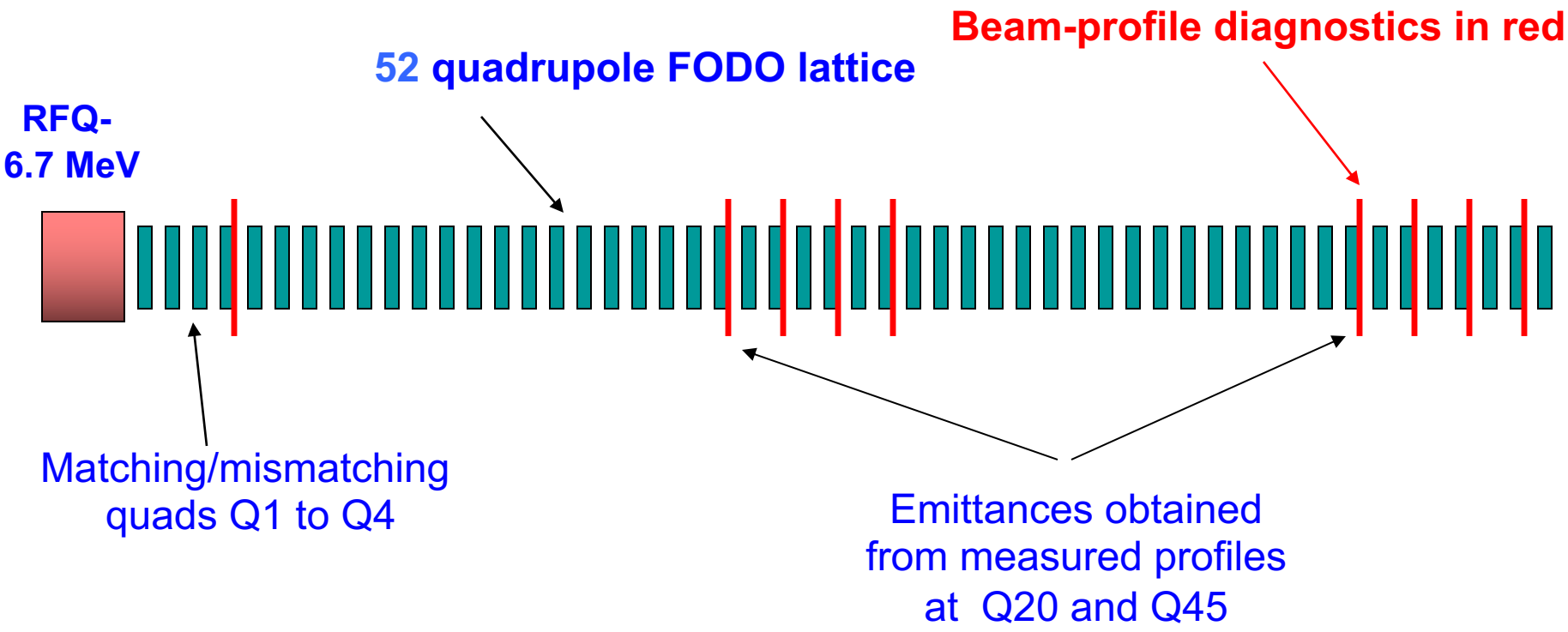

LANL Beam Halo Experiment Lattice

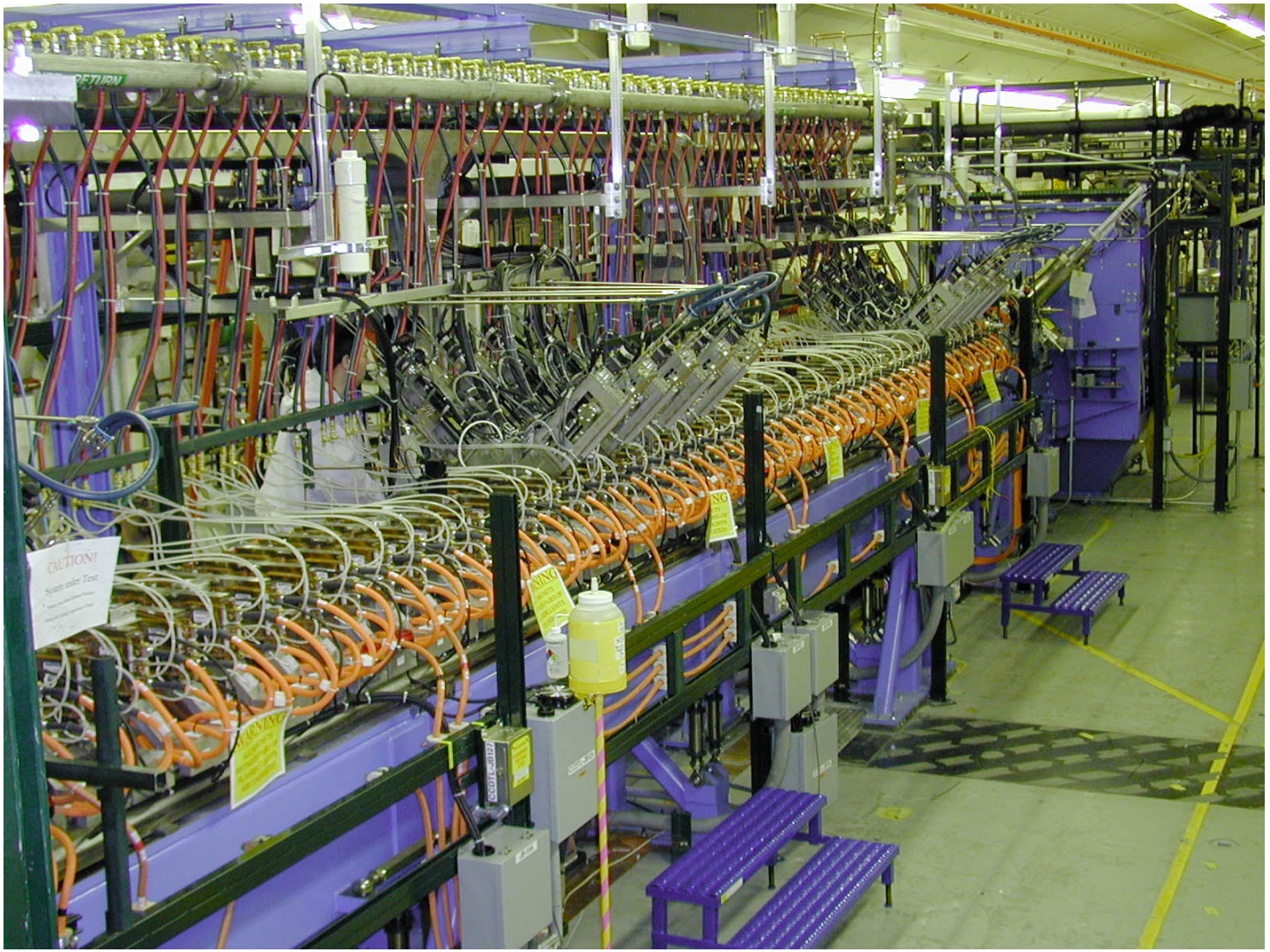

Wire and Scraper Beam-Profile Diagnostic to Measure Beam Profile

- 33-micron carbon wire (too thin to be visible in picture) measures density in beam core above 10^{-3} level.
- Proton range=300 microns so protons pass through wire and make secondary electrons to measure high density in beam core.
- Pair of 1.5mm graphite scraper plates in which protons stop. Can measure proton density outside beam core from 10^{-3} to 10^{-5}.
- Data from wire and scraper plates were combined to produce a single distribution.

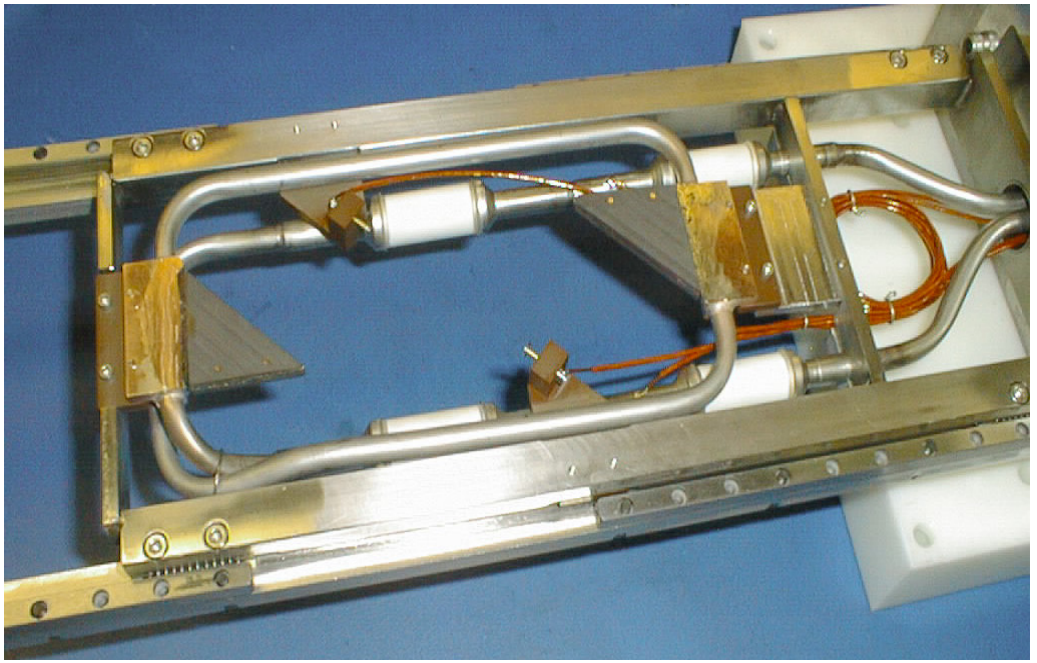

Measured Beam Profile

Typical matched beam profile for 75 mA. (μ=1,matched)

Shows Gaussian-like core plus low-density halo input beam, observed out to 9 rms.

Linear Plot

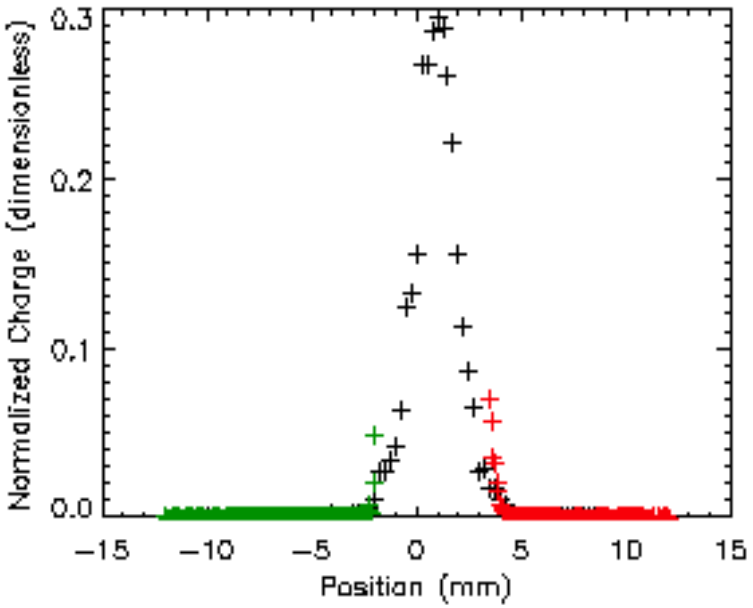

Semilog Plot

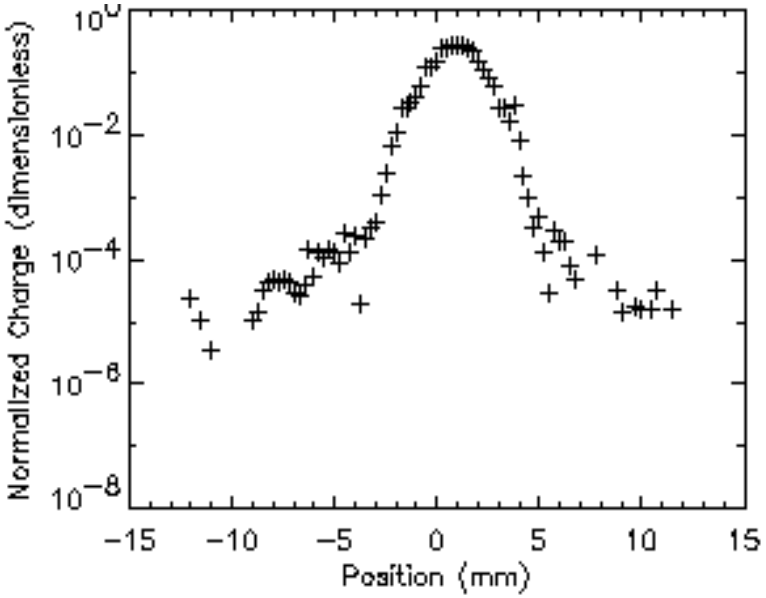

Beam Emittance Growth

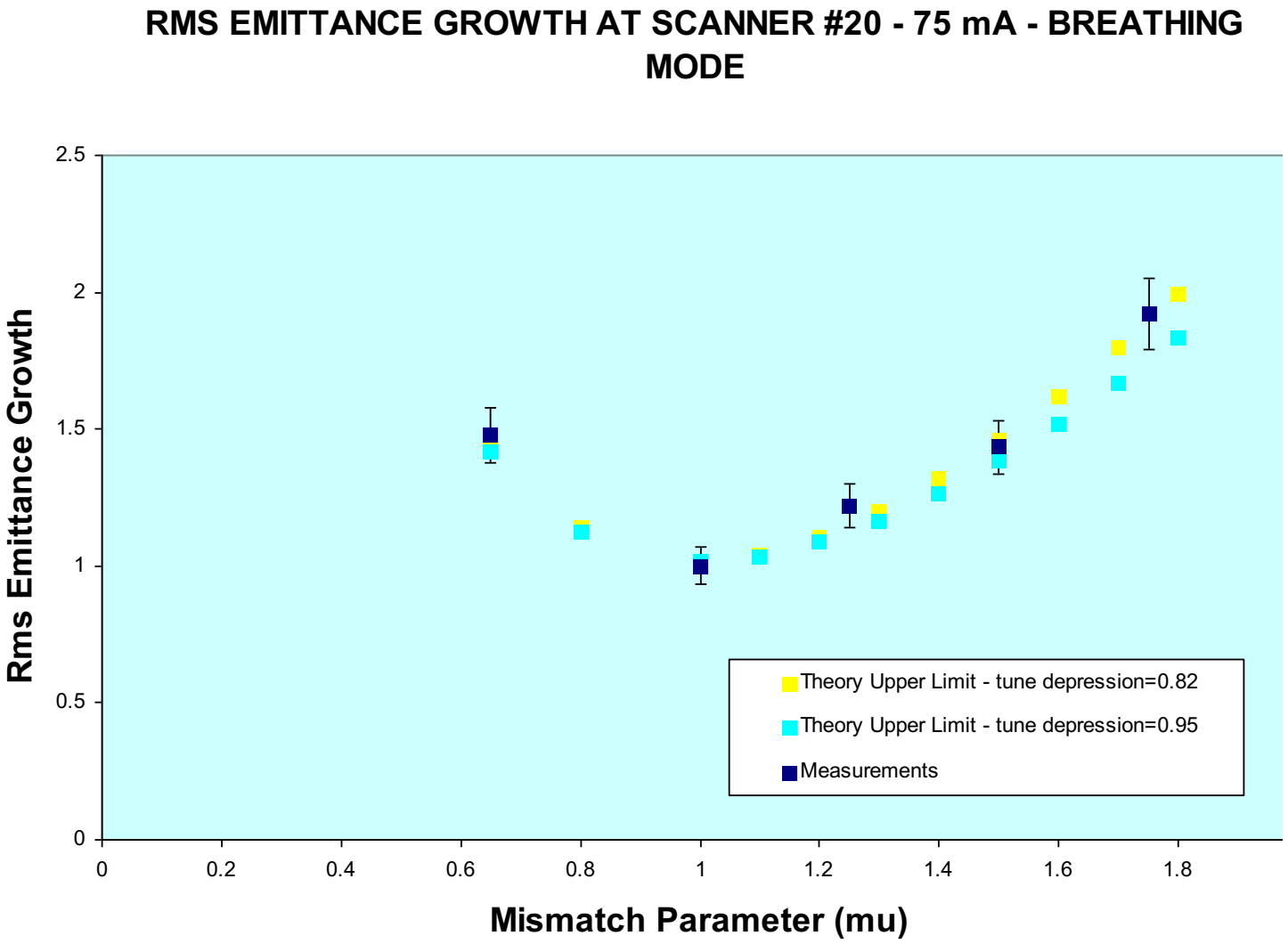

Test of Particle-Core Model Measurements at Different Fractional Intensity Levels (10%, 1%, 0.1%)

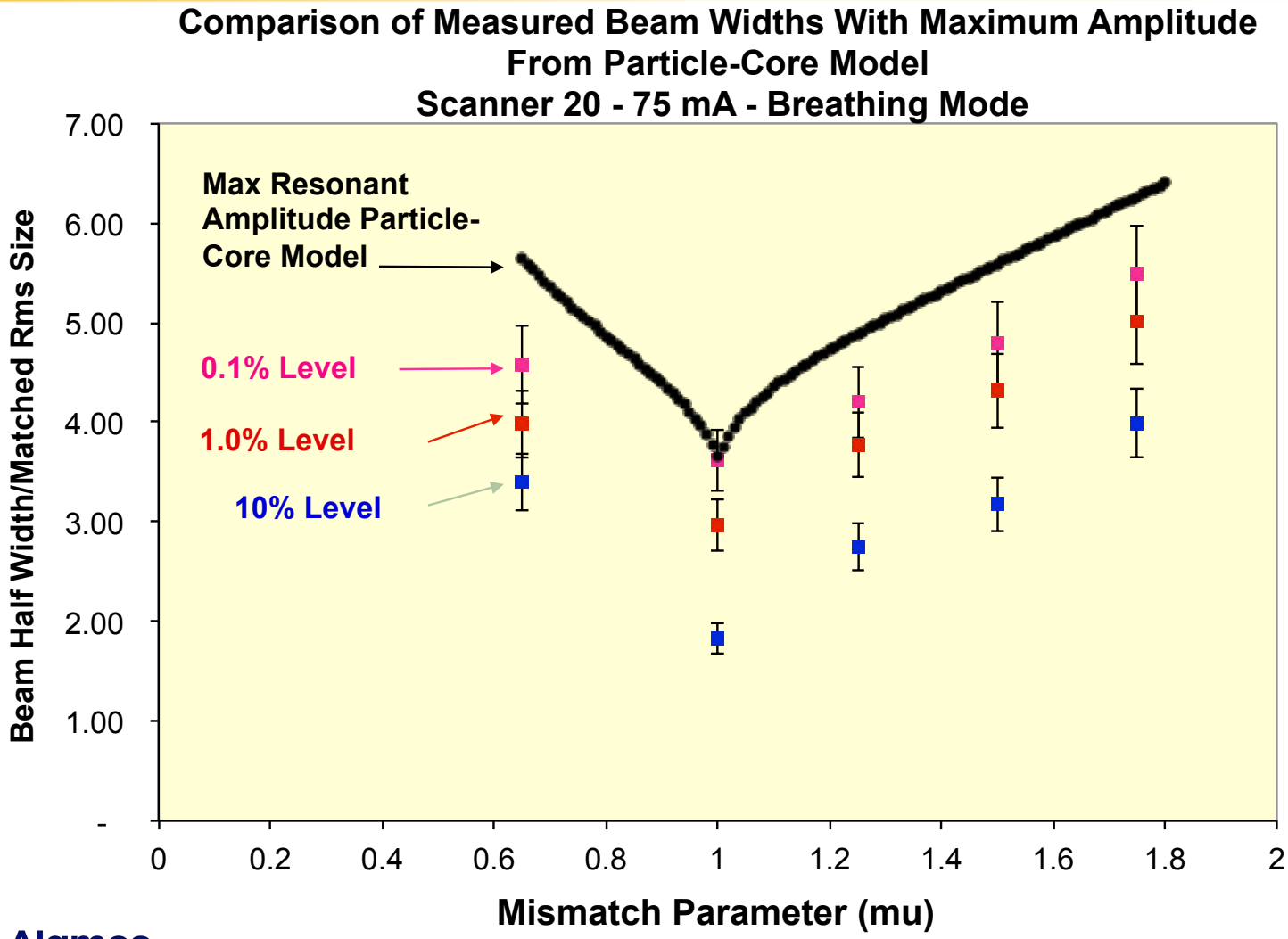

Instability of Anisotropic KV Beam

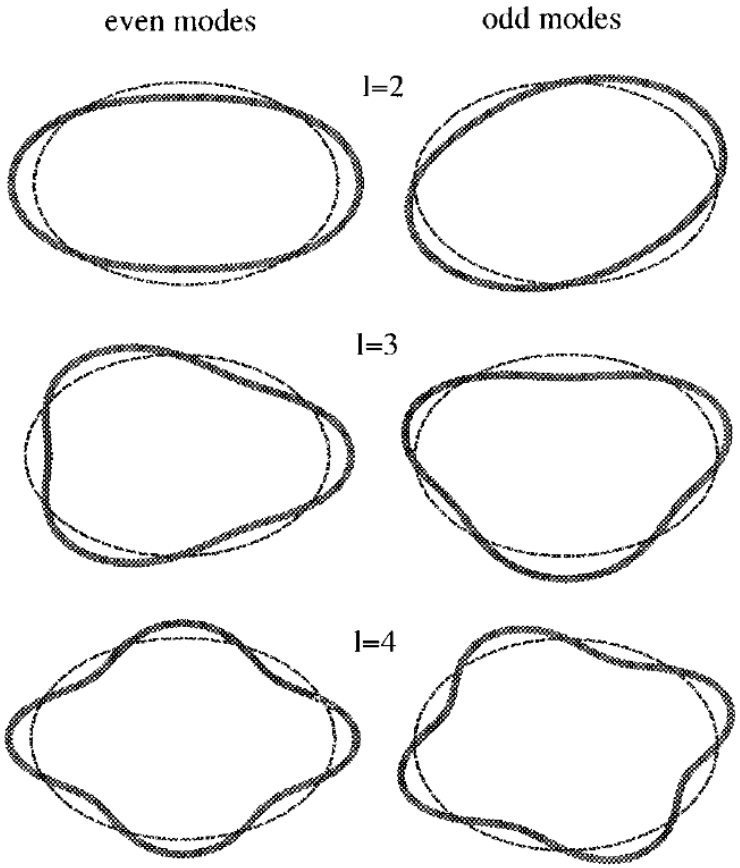

KV Beam with unequal emittances in a focusing channel with different focusing strength in x- and y- directions

$$f_0(x,y,p_x,p_y)=\frac{NT\nu_y/\nu_x}{2\pi^2 m\gamma a^2}\,\delta(H_{0x}+TH_{0y}-m\gamma\nu_x^2a^2/2)$$

Ratio of beam emittances:

$$\frac{\epsilon_x}{\epsilon_y}=\frac{a^2\nu_x}{b^2\nu_y}$$

Beam cross sections for second, third and fourth order even and odd modes ~schematic, with x horizontal and y vertical coordinates.

(I.Hofmann, 1998)

Instability of Anisotropic KV Beam (cont.)

Perturbed distribution function

$$f \equiv f_0(H_{0x}, H_{0y}) + f_1(x, y, p_x, p_y, t)$$

Vlasov's equation for perturbed beam distribution function

$$\frac{df_1}{dt} \equiv \frac{\partial f_1}{\partial t} + \frac{p_x}{m\gamma}\frac{\partial f_1}{\partial x} + \frac{p_y}{m\gamma}\frac{\partial f_1}{\partial y} - m\gamma\nu_x^2 x\frac{\partial f_1}{\partial p_x} - m\gamma\nu_y^2 y\frac{\partial f_1}{\partial p_y}$$

$$= \frac{NTq\,\nu_y/\nu_x}{2\pi^2 m^2\gamma^4 a^2}\left(p_x\frac{\partial\Phi}{\partial x} + Tp_y\frac{\partial\Phi}{\partial y}\right)$$

$$\times\,\delta'[p_x^2 + \nu_x^2 x^2 + T(p_y^2 + \nu_y^2 y^2) - \nu_x^2 a^2]. \qquad (11)$$

Poisson's equation for perturbed electrostatic potential created by perturbed space charge density

$$\nabla^2\Phi = -\frac{q}{\epsilon_0}n_1 = -\frac{q}{\epsilon_0}\int f_1 dp_x dp_y .$$

Instability of Anisotropic KV Beam

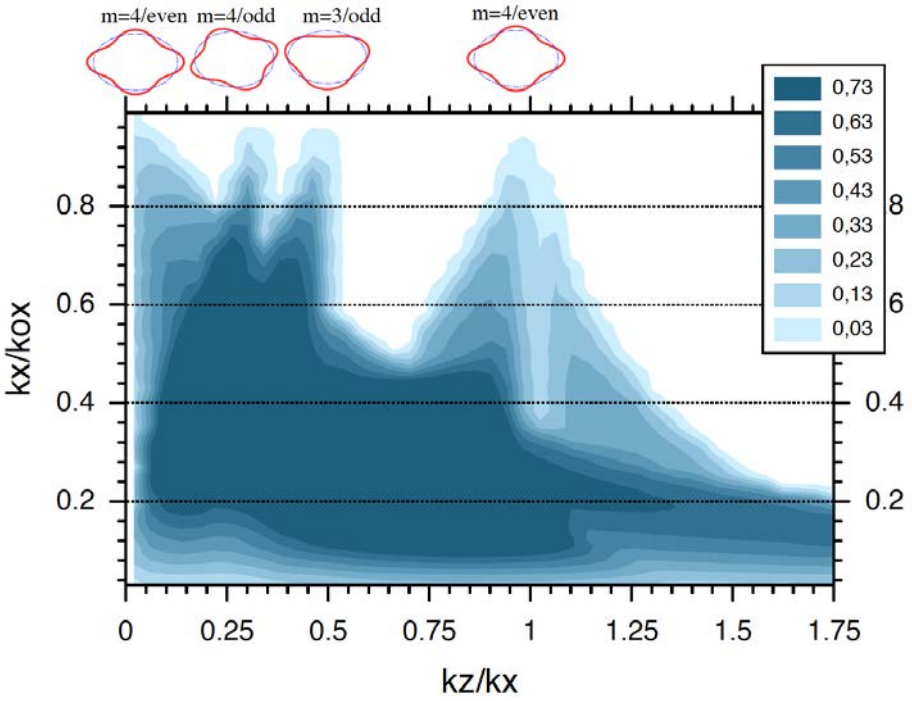

Stability chart for $\varepsilon_z/\varepsilon_x=0.5$.

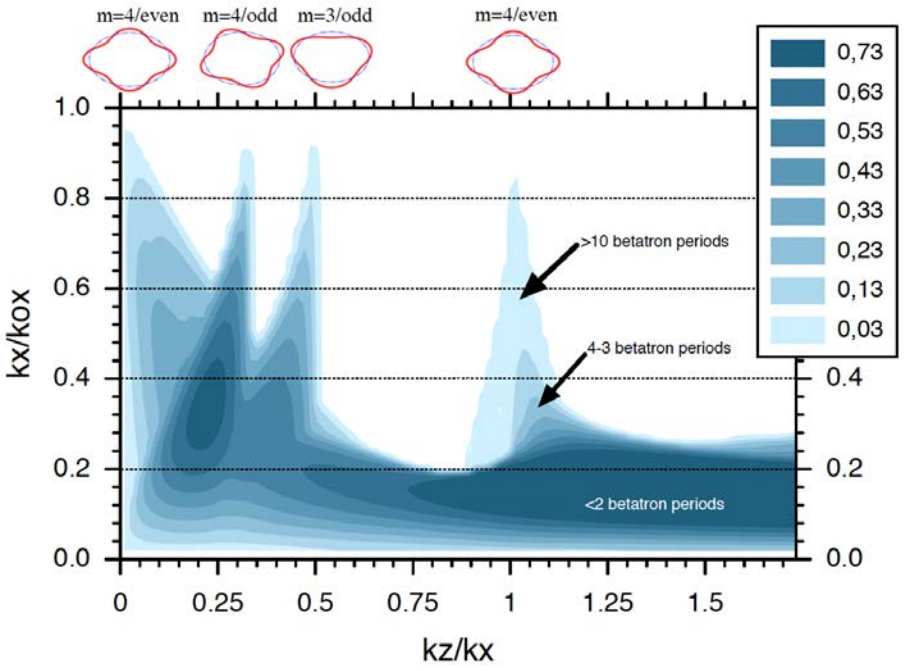

Stability chart for $\varepsilon_z/\varepsilon_x=1.2$.

Stability charts derived for KV beam with different transverse emittances in focusing channels with different focusing strengths in two transverse directions. Charts are applied to motion in RF field assuming one direction (x-) in transverse and another (z-) is longitudinal.

Instability of Anisotropic KV Beam

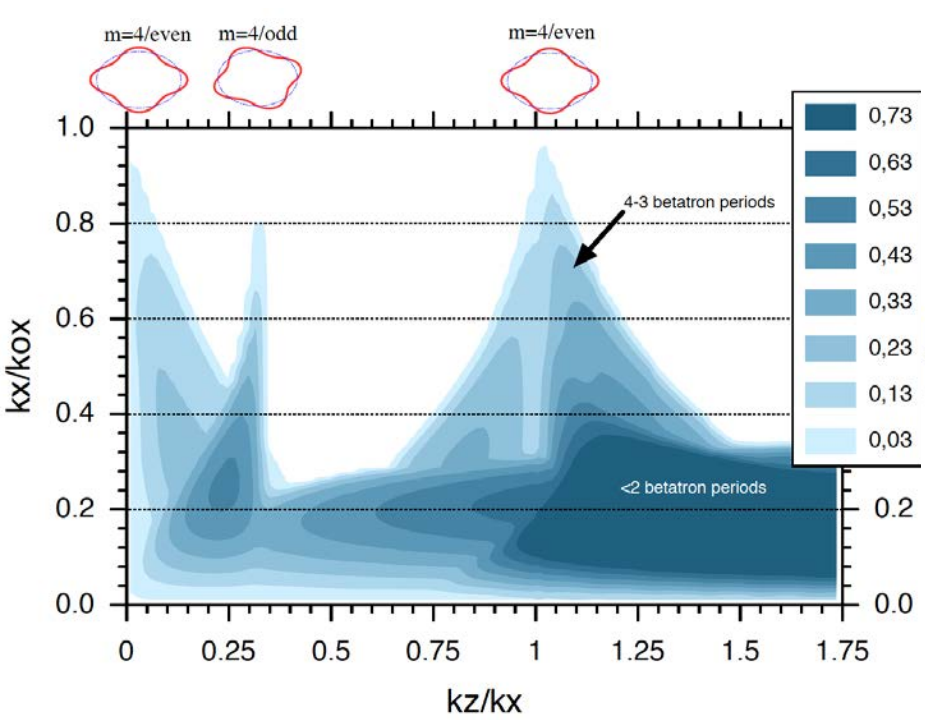

Stability chart for $\varepsilon_z/\varepsilon_x$=2.0.

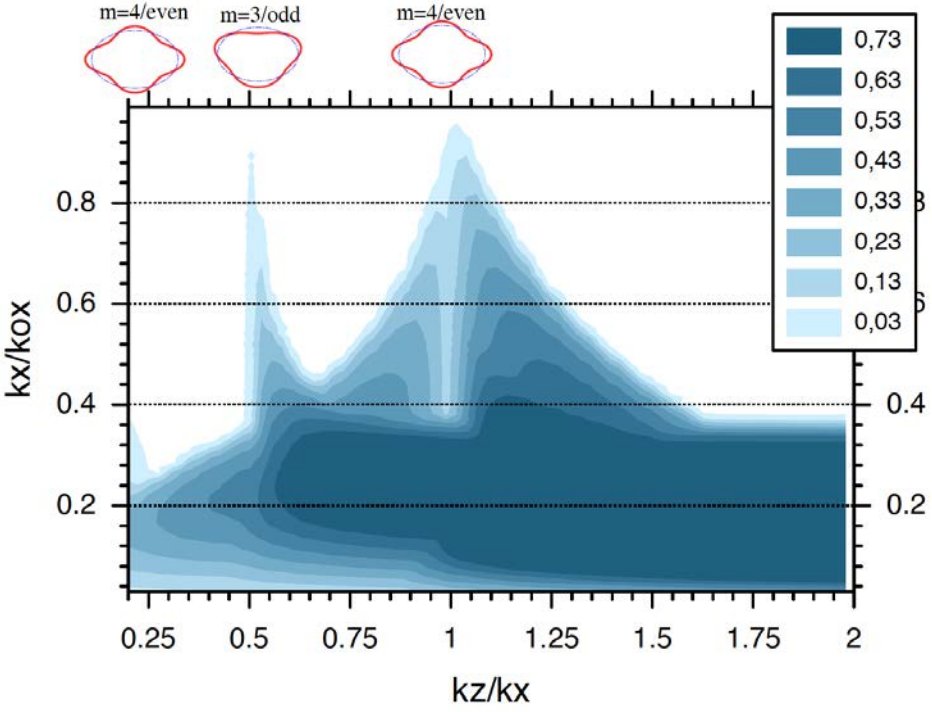

Stability chart for $\varepsilon_z/\varepsilon_x$=3.0.

Instability of Anisotropic KV Beam

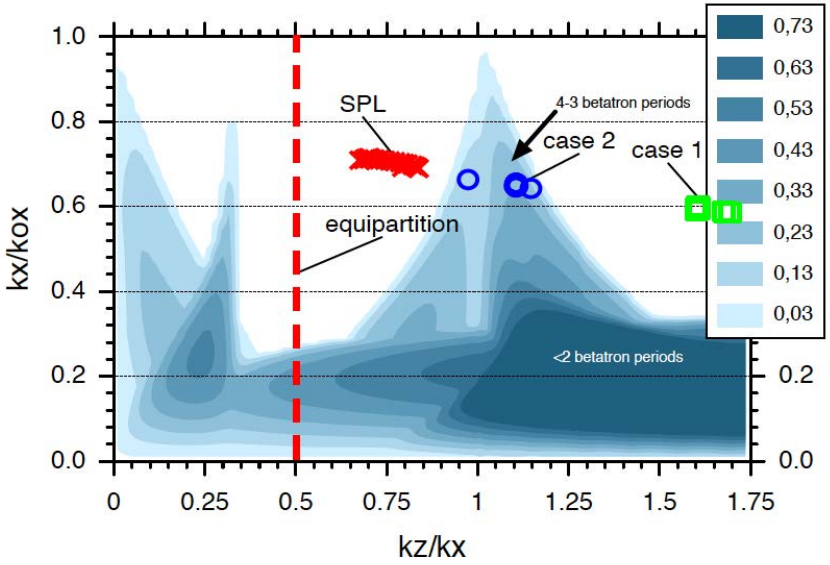

Stability chart for $\varepsilon_z/\varepsilon_x$=2.0.

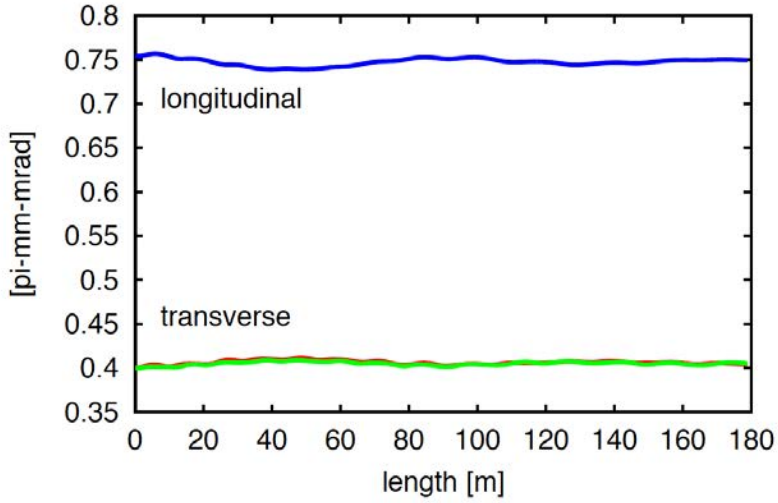

Rms emittance evolution for SPL lattice.

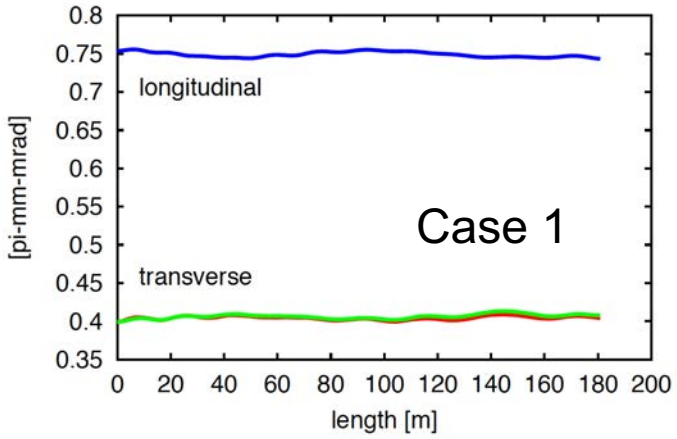

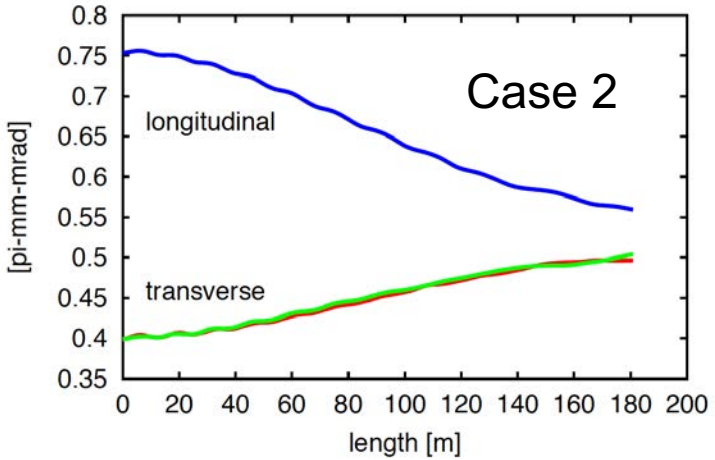

Rms emittance evolution

Experimental Verification of Stability Charts

(C.Plostinar et al, IPAC2013)

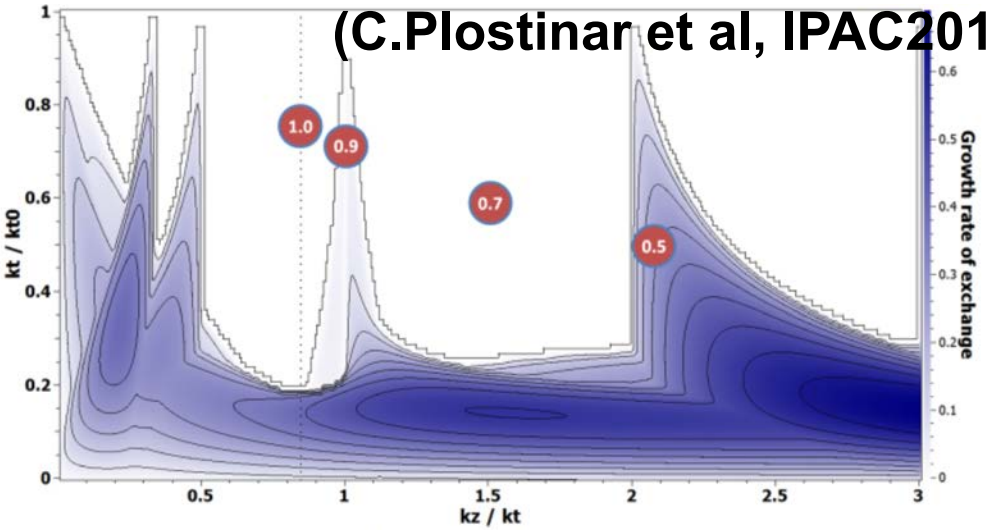

Figure 2: J-PARC linac stability chart for an emittance ratio $\varepsilon_z/\varepsilon_t = 1.2$. Dotted is the EQP line.

Table 2: Measured emittance values at SDTL15.

T_t/T_z	ε_t (π.mm.mrad)	ε_z (π.mm.mrad)
1.0	0.216	0.269
0.9	0.229	0.233
0.7	0.253	0.223
0.5	0.293	0.161

Single-particle parametric resonances:
k_z / k_x = 2/3, 1, 2.

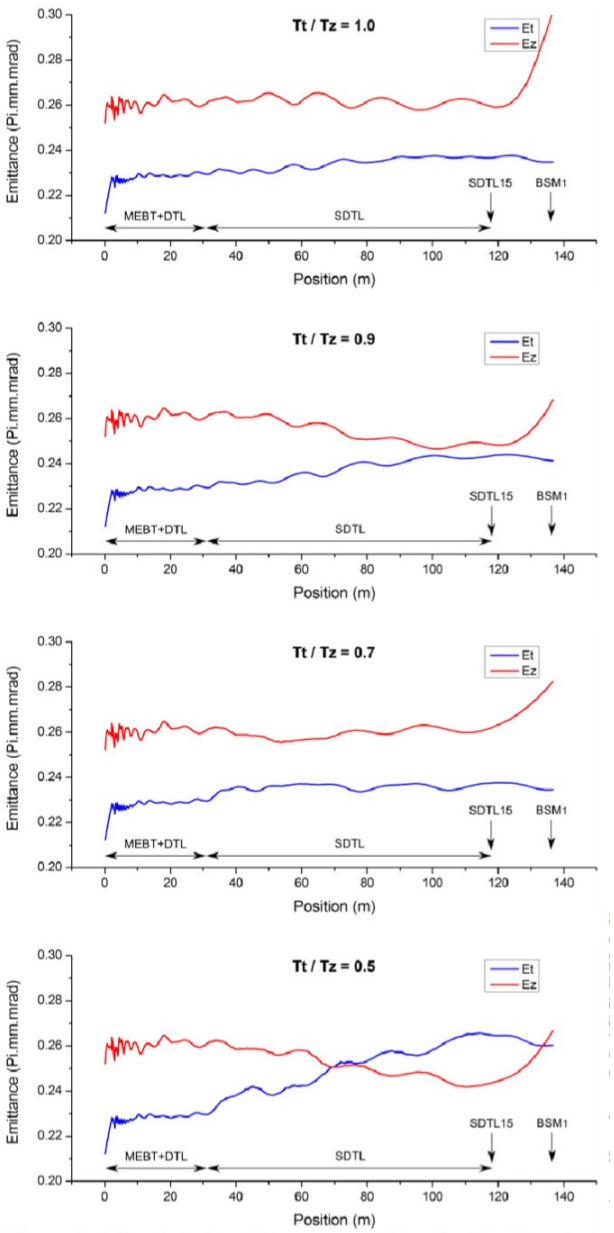

Figure 3: Simulated emittance evolution for the four test cases (RMS Normalised).